

# A History of Collapse Factor Modeling and Empirical Data for Cryogenic Propellant Tanks

Laurence de Quay<sup>\*</sup>

*NASA Stennis Space Center, MS, 39529, USA*

B. Keith Hodge<sup>†</sup>

*Mississippi State University, MS, 39762, USA*

One of the major technical problems associated with cryogenic liquid propellant systems used to supply rocket engines and their subassemblies and components is the phenomenon of propellant tank pressurant and ullage gas collapse. This collapse is mainly caused by heat transfer from ullage gas to tank walls and interfacing propellant, which are both at temperatures well below those of this gas. Mass transfer between ullage gas and cryogenic propellant can also occur and have minor to significant secondary effects that can increase or decrease ullage gas collapse. Pressurant gas is supplied into cryogenic propellant tanks in order to initially pressurize these tanks and then maintain required pressures as propellant is expelled from these tanks. The net effect of pressurant and ullage gas collapse is increased total mass and mass flow rate requirements of pressurant gases. For flight vehicles this leads to significant and undesirable weight penalties. For rocket engine component and subassembly ground test facilities this results in significantly increased facility hardware, construction, and operational costs. "Collapse Factor" is a parameter used to quantify the pressurant and ullage gas collapse. Accurate prediction of collapse factors, through analytical methods and modeling tools, and collection and evaluation of collapse factor data has evolved over the years since the start of space exploration programs in the 1950's. Through the years, numerous documents have been published to preserve results of studies associated with the collapse factor phenomenon. This paper presents a summary and selected details of prior literature that document the aforementioned studies. Additionally other literature that present studies and results of heat and mass transfer processes, related to or providing important insights or analytical methods for the studies of collapse factor, are presented.

## I. INTRODUCTION

Following initial developmental work in the 1920's and 1930's by Robert H. Goddard, liquid propellant rockets have been further developed and utilized extensively for military missile, earth-to-orbit launch system, and space propulsion-system applications. The vast majority of larger high thrust (greater than 44,000 N or 10,000 lb) liquid propellant rockets utilize one or more cryogenic liquid propellants because of the high combustion-energy-to-mass ratio or high combustion energy to volume ratio provided with these types of propellants.

The more than 80-year history of liquid propellant rockets has been a series of continuous improvements in propulsive efficiency, increased thrust levels, significant increases in thrust-to-weight ratios, and an expanding variety of engine cycles.

Initiatives starting in the late 1980's have placed the emphasis on reduction of costs with improved reliability and safety in the manufacture, ground testing, and operation of all rocket propulsion systems. Further development initiatives starting in the middle 1990's have included renewed interest in liquid-oxidizer-solid-fuel (hybrid) rocket motors and liquid propellant rocket engines with oxidizer-rich, staged-combustion power cycles or unchoked low differential pressure propellant injectors. These initiatives have necessitated the use of ground test facilities with cryogenic run systems operating at high subcritical and supercritical pressures.

---

<sup>\*</sup>Aerospace Engineer, NASA/SSC Mail Stop EA33, SSC, MS, Associate Fellow

<sup>†</sup>Professor of Mechanical Engineering, Mail Stop 9552, Mississippi State, MS, Associate Fellow

## A. Flight Vehicles

All flight vehicles propelled by liquid propellant and hybrid rocket engines require one or more pressurized propellant tanks in which propellant is expelled from tanks to supply one or more rocket engines. A simplified schematic of a pump fed liquid propulsion system, which employs one of the simple basic power cycles, is shown in Figure 1. In this system, turbopumps boost the pressures of propellants supplied from the propellant tanks such that these propellants can be injected into the rocket engine's thrust (main combustion) chamber denoted in the Figure.

Figure 1 is obtained from Ref. 1 and a more detailed discussion about liquid propellant rockets is also presented in this reference.

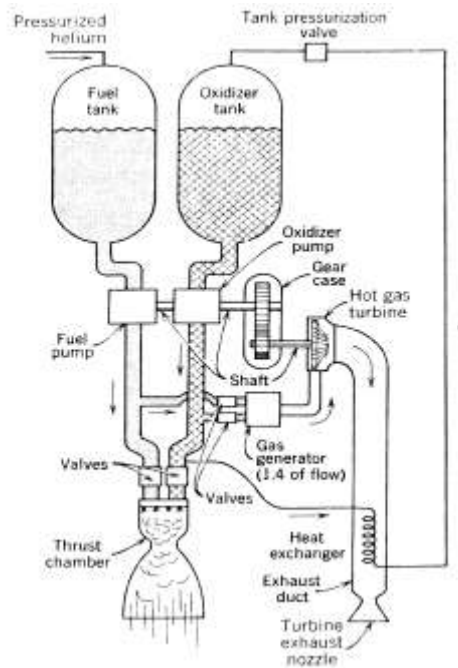


**Figure 1. Simplified Schematic of a Typical Pump Fed Liquid Rocket Propulsion System (Gas Generator Cycle, Single Turbine Driving Both Turbopumps)**

## B. Ground Test Facilities

A key and critical component for design concept evaluation, development, flight certification, and subsequent use of rocket propulsion systems is the ground testing of rocket engine assemblies, subassemblies, and components as well as integrated rocket stages and major segments of the flight vehicle. The ground testing of individual rocket engine components and subassemblies during the early stages of development has been given increased attention and importance due to the aforementioned cost reduction and reliability and safety enhancement initiatives started in the late 1980's. Additionally, increased complexity and higher propulsion system pressures associated with a number of recent liquid propellant rockets to increase propulsive efficiency has emphasized the importance of rocket engine component and subassembly ground testing.

For the majority of high-thrust liquid propellant rocket engines and hybrid rocket motors, where one or more pressurized cryogenic propellants are used, a high fidelity and performance ground testing facility is essential. This facility normally operates one to three low- and high-pressure cryogenic propellant feed (run) systems that supply propellants to rocket engine assembly, subassembly, or component test articles at required interface pressures and

mass flow rates. For the cases where rocket engine subassemblies and components, such as turbopumps and combustion devices, are ground tested, at least one of the test facility cryogenic propellant run systems operates at high subcritical or supercritical pressures. (Critical pressures for oxygen, nitrogen, and hydrogen are 187.5-psia, 493.0-psia, and 731.2-psia respectively.) In all cases, the ground testing facility is required to simulate the remaining propulsion system or flight vehicle by providing required propellant pressures, mass flows, and temperatures at main fluid interfaces of the component being tested.

Figure 2 shows a simplified schematic of a ground test facility cryogenic propellant feed system, which supplies propellant to a typical interface on a test article.

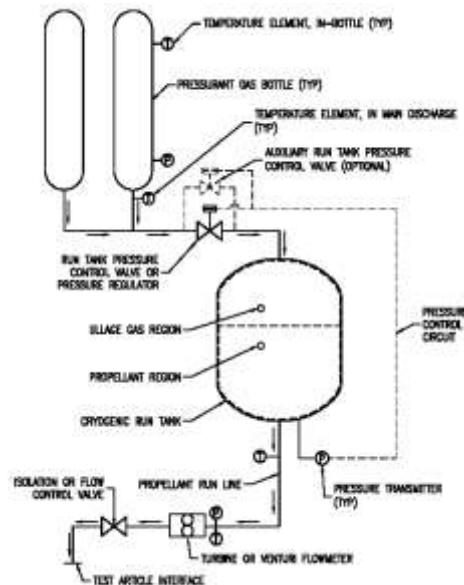


Figure 2. Simplified Schematic of a Cryogenic Propellant Feed System

### 1. Cryogenic Run Tank

The main component of the cryogenic propellant feed (or run) system is the cryogenic propellant run tank. This component serves as the system reservoir where liquid or cold supercritical cryogenic propellant; typically liquid oxygen, liquid hydrogen, or liquid methane; is expelled under pressure at the main discharge nozzle. This propellant is conveyed via a cryogenic propellant run system, comprised of series of pipelines that generally includes valves, filtration device, and flow meter(s), to one or more of the test article interfaces. The cryogenic run tank main discharge nozzle is located at or near the lowest point of the tank such that nearly all propellant can be expelled from the tank.

Referring to Figure 2, the internal volume of the cryogenic run tank is comprised of two regions, the propellant region and the ullage-gas region.

Pressurant gas needs to be supplied into the ullage gas region as the volume or internal pressure of this region increases. This pressurant gas is normally supplied by one of two methods. In one method, called the autogenous tank pressurant gas supply method, a portion of the liquid or supercritical cryogen exiting the main discharge of the run tank is vaporized or heated by a heat exchanger and is then routed into the tank ullage region at one or more entry points near the top of the tank. For the other method, called the external pressurant gas supply method, pressurant gas is supplied into the tank ullage externally from one or more gas bottles or other sources.

For cryogenic propellant run systems used on ground testing facilities, the external pressurant gas supply method is generally employed. Pressurized gas bottles, as shown in Figure 2, provide this gas via a series of pipelines and components to the cryogenic run tank ullage.

## 2. *Pressurant Gas Subsystem*

The pressurant gas subsystem supplies all or most of the additional gas needed in the run tank ullage for maintaining required cryogenic run tank pressures as propellant is expelled from the tank. The pressurant gas subsystem is depicted as the gas bottles and pipelines with associated components between these bottles and the cryogenic run tank ullage gas region in Figure 2.

## 3. *Heat and Mass Transfer Processes in the Cryogenic Run Tank*

Unique heat and mass transfer processes occur in cryogenic propellant tanks. These tanks (and flight vehicle propellant tanks) have propellant regions and tank walls that are generally tens to hundreds of degrees R colder than most of the ullage and the pressurant gases that enter the ullage gas regions. This results in significant rates of heat transfer from the ullage gas region to tank walls and the cryogenic propellant. Subsequently this heat transfer reduces the temperatures of the ullage gas region, thereby causing its mean density to increase (as compared to the ideal condition where negligible heat transfer takes place). This increase in mean ullage gas density is known as ullage gas collapse and has the net effect of increasing the mass flow rate and total mass accumulation of pressurant gas entering the cryogenic run tank ullage.

### **C. Collapse Factor**

An important parameter, "Collapse Factor," has been defined and used in much of the literature as a measure of performance for the process in which a pressurant gas is transferred into the ullage of a cryogenic propellant tank in order to maintain and control pressures in the tank.

"Collapse Factor" is defined as the ratio of actual-to-ideal pressurant gas requirements for both tank pressurization and pressurized propellant expulsion from a cryogenic propellant run tank. There are two types of collapse factor that are defined as performance metrics when designing, analyzing, or evaluating pressurant gas subsystems used for cryogenic run tanks. These are "Instantaneous Collapse Factor" and "Cumulative Collapse Factor." Instantaneous collapse factor is defined as the ratio of pressurant gas mass flow rate into a cryogenic propellant run tank under actual conditions to the mass flow rate under ideal conditions. Cumulative collapse factor is defined as the total mass of pressurant gas transferred into the cryogenic propellant tank under actual conditions divided by the total mass of this gas transferred under ideal conditions. For both types of collapse factors, the ideal conditions are based on and derived under the following assumptions:

- 1.) Negligible heat transfer at ullage gas and propellant region boundaries,
- 2.) Propellant and ullage gas occupy two distinct regions in the tank,
- 3.) Propellant region and ullage gas region are each at uniform temperatures,
- 4.) Pressurant gas that enters the ullage gas region is uniformly mixed with ullage gas in this region,
- 5.) Mass transfer across the interface between the propellant and the ullage gas is negligible,
- 6.) The ullage gas region has a uniform mixture ratio of gases if more than one species of gas is present in the region.

### 1. *Importance of Collapse Factor*

The collapse factor during each operation of a cryogenic propellant tank has a direct effect on the required sizing and design of the pressurant gas subsystem described in Section I.B.2. The proper sizing and design of this subsystem to provide the needed total mass transfer and flow rates of pressurant gas into the run tank ullage for all operating conditions is very critical for both flight vehicles and ground testing facilities. An undersized subsystem results in system or flight vehicle mission failure as the propellant mass flow rate out of the tank cannot be maintained for the required time durations. Conversely, an oversized pressurant gas subsystem results in significant construction and operational cost impacts with no beneficial returns. For flight vehicles, the severe penalty of added weight also exists with an oversized pressurant gas subsystem.

## II. Empirical Collapse Factor Data

Since the late 1950's, a wide variety of collapse factor data have been obtained. Table 1 presents a sampling of empirically-obtained collapse factors for tank pressurization and pressurized tank expulsion of liquid oxygen (LOX), liquid methane (LCH<sub>4</sub>), and liquid nitrogen (LN). Table 2 reviews empirical collapse factor data from tank pressurization and pressurized tank expulsion of liquid hydrogen (LH) and slush hydrogen (SLH) propellants. In both Tables 1 and 2, other data are presented in addition to collapse factors to provide an indication of the variety and range of propellant tank and interfacing system conditions associated with the range of collapse factor values. Unless noted otherwise, all empirical collapse factors in Tables 1 and 2 are cumulative collapse factors at the end of tank expulsion where single values are listed. Where a range of collapse factor values is presented, this range defines the minimum and maximum cumulative collapse factors between the start of propellant expulsion from the tank and the end of this expulsion process, unless noted otherwise on the tables.

Perhaps the most important and significant observation from the empirical collapse factor data is the paucity of empirical data for supercritical and high subcritical tank pressure conditions. Only four tests, from References 3 and 8 in Tables 1 and 2, are conditions where tank pressures are above the critical pressures of the LOX propellant. The data from References 2, 14, and 15 have tests where high subcritical tank pressure conditions existed during tests. Another test from Reference 8 also had a high subcritical pressure tank pressure condition for an LN tank expulsion.

## III. Phenomena Affecting Collapse Factor

There are various observed phenomena during the operation of cryogenic propellant tanks that appear to have significant influences on empirical collapse factors. These include properties distributions within the ullage gas, liquid or cold supercritical propellant, and tank walls. The predominant property where spatial distribution has significant effects is temperature. The spatial distribution of mass fraction of constituent fluids in the ullage gas and propellant regions can also have non-negligible effects on collapse factors under certain operating conditions.

### A. Ullage Gas Region Properties Distribution

One of the most important and influential attributes of a cryogenic propellant tank system with respect to collapse factors during tank pressurization and pressurized propellant expulsion processes is the variation and distribution of fluid properties within the ullage gas region. The variation of ullage gas properties is mainly due to temperature gradients in the ullage gas region as pressures vary very little because of low ullage gas densities, short vertical tank (and maximum ullage gas region) heights, and ullage gas elevation head pressures being small in comparison to absolute tank pressures.

For selected cases where propellant and pressurant gas are different species and where significant levels of mass transfer of propellant species into and within the ullage gas region are occurring, the distribution of propellant species mass fraction within the ullage gas region can also have an effect on the distribution of fluid properties in the ullage gas region. The observed dominant effect of temperature on the distribution of ullage gas properties is primarily due to the relatively short time durations of typical tank pressurization and propellant expulsion processes as well as the natural stability of the fluid regions inside the tank where fluid temperatures decrease and fluid densities increase when traversing from the top to the bottom in the tank.

Regarding the literature, there are a number of empirical tests where temperatures are measured at many discrete locations in the ullage gas region of cryogenic propellant tanks. These measurements have been recorded at discrete times through tank pressurization and pressurized propellant expulsion processes. Unfortunately, there are no ullage gas region temperature distribution data for supercritical tank pressure conditions and no practicable methods exist to obtain these data at the high supercritical pressures. Previous attempts to utilize insitu instruments inside cryogenic propellant tanks at supercritical pressures, necessary to obtain accurate temperature measurements of fluids inside the tank, have resulted in unreliable data from, severe damage to, or destruction of these types of instruments.

**Table 1 Selected Empirical Collapse Factor Data for Non-Hydrogen Propellant Tanks**

Reference Citation	Test Run #	Tank Volume (gallons)	Tank Shape	Prop.	Propellant Expulsion			Pressurant Gas		Notes	Empirical Collapse Factor	
					Mass Flow Rate (lb/sec)	Vol. Flow Rate (gpm)	Time (sec)	Tank Press. (psia)	Species			Inlet Temp. (deg R)
2	None	25	Cylindrical	LN	10.0 - 14.0	88.9 - 124.3	16	172.3 - 300.4	He	523 - 530	(1)	1.540
2	None	25	Cylindrical	LN	10.0 - 14.0	88.9 - 124.3	16	155.2 - 321.6	Steam/He	1938 - 2029	(1), (2)	1.510
3	0027A	2603	Sphere	LOX	340-382	2066 - 2338	47	4400 - 5550	GN	579 - 521	(3)	1.061 ± 0.060
3	0029B	2603	Sphere	LOX	462-478	2768 - 2873	15.2	7600 - 8200	GN	579 - 531	(4)	1.054 ± 0.054
4	36	489.5	Sphere	LCH <sub>4</sub>	3.62	61.5	389.2	49.3	He	407		1.769
4	41	489.5	Sphere	LCH <sub>4</sub>	3.625	61.5	390.3	49.5	He	407		2.431
4	40	489.5	Sphere	LCH <sub>4</sub>	2.332	39.5	598.5	49.5	He	596		2.423
4	6	489.5	Sphere	LCH <sub>4</sub>	2.244	38.1	632.8	49.5	GCH <sub>4</sub>	407		2.352
4	11	489.5	Sphere	LCH <sub>4</sub>	6.137	104.6	233.5	49.2	GCH <sub>4</sub>	608		2.550
4	99	489.5	Sphere	LCH <sub>4</sub>	3.823	65.1	377.7	49.5	GN	603	(5)	5.247
5	See Notes	11220	Oblate Spheroid	LOX	201.2	1267.4	478	~46	He	325	(10)	1.375
5	See Notes	94996	Oblate Spheroid	LOX	2230 - 2256	14047 - 14227	360	36. - 37.5	GOX	510	(11)	1.325 - 1.500
6	12B	2596	Oblate Spheroid	LOX	57.7	363.5	47	34	He	520		2.432
6	13A	2596	Oblate Spheroid	LOX	57.7	363.5	120	34	He	527		2.605
6	10	2596	Oblate Spheroid	LOX	57.7	363.5	415	34	He	255		1.304
6	14A	2596	Oblate Spheroid	LOX	57.7	363.5	242	40	He	525		1.961
7	?	59892	Multi-Cylinder	LOX	3767 - 3769	23740	114.5	60 - 80	GOX/GN	840 - 600	(6), (7), (8)	~1.700
7	?	10098	Cylindrical	LOX	1261	7943	70	68 - 76	GOX/GN	602 - 641	(7), (8)	~1.650
7	?	16.5	Cylindrical	LN	0.924	8.21	120	50	GN	530	(7)	~2.110
8	74	5000	Cylindrical	LN	30. - 525.	267. - 4729.	38	335. - 359.	GN	506 - 447		2.35 - 1.39
8	74	900	Sphere	LOX	10.2	61.5	26	8200 - 8300	GN	548 - 544	(9)	4.1 - 1.57

- Notes:
- (1) Assumed near constant ullage gas temperature and no GN in ullage for expulsion
  - (2) Tank pre-pressurized with helium prior to expulsion with steam as pressurant gas
  - (3) Time includes ~3 sec. main ramp up in propellant expulsion mass flow rate and tank pressure; indicated tank pressure and flow rates do not include this ramp up
  - (4) Time includes ~5 sec. main ramp up in propellant expulsion mass flow rate and tank pressure; indicated tank pressure and flow rates do not include this ramp up
  - (5) Data shows 69.3% of added GN pressurant gas dissolved into upper layer of LCH<sub>4</sub> propellant
  - (6) Multiple tanks with 4-each 70-inch diameter tanks connected to one-each central 105-inch diameter tank
  - (7) Collapse factors approximated using energy allocations for ullage gas; insufficient data for more exact computations
  - (8) Tank pre-pressurized with GN prior to using GOX for propellant expulsion
  - (9) Only last 26-seconds of 38-second run has reliable data
  - (10) Propellant expulsion flowrate based on assumed 10% initial ullage and complete emptying of propellant from tank; test run is from unpublished document cited in Ref. 5
  - (11) Tank pressure and LOX expulsion rate obtained from Ref. 9 using average summations of LOX flow rate to 5-each J-2 engines on S-II stage; test run is from unpublished document cited in Ref. 5

Table 2 Selected Empirical Collapse Factor Data for Hydrogen Propellant Tanks (Continued on Next Page)

Reference Citation	Test Run #	Tank Volume (gallons)	Tank Shape	Prop.	Propellant Expulsion			Pressurant Gas			Empirical Collapse Factor	
					Mass Flow Rate (lb/sec)	Vol. Flow Rate (gpm)	Time (sec)	Tank Press. (psia)	Species	Inlet Temp. (deg R)		Notes
3	004A	5002.5	Sphere	LH	78 - 108	6100 - 8560	34	7450 - 8200	GH	619 - 549	(1)	1.047 ± 0.037
5	See Notes	49,472	Sphere	LH	60.84	6140.5	296	91.7	GH	530	(16)	1.64
5	See Notes	246,840	Multi-Cylinder	LH	391.4 - 394.1	39696 - 39970	360	28.5 - 30.0	GH	200	(7), (16)	1.15 - 1.25
10	B-1	12	Cylindrical	LH	Not Given	Not Given	62.4	39.25	GH/He	330	(2)	3.42
10	B-2	12	Cylindrical	LH	Not Given	Not Given	62.4	39.25	GH/He	265	(2)	2.16
10	B-1	12	Cylindrical	LH	No Expulsion	N/A	N/A	14.7 - 44.25	GH	505		4.45
10	B-1	12	Cylindrical	LH	No Expulsion	N/A	N/A	14.7 - 61.75	GH	295		3.26
10	2	500	Cylindrical	LH	2.561	259.4	100	45.5	GH	320	(3), (4)	2.23
10	5	500	Cylindrical	LH	2.031	205.7	99	45.5	He	300	(3), (4)	1.72
10	7	500	Cylindrical	LH	2.031	205.7	105	49.3	GH	300	(3), (5)	1.74
10	10	500	Cylindrical	LH	1.833	185.7	111	45	GH	300	(3)	1.74
11	3	~370	Cylindrical	LH	0.939	95.1	197	44.1	He	450	(6)	0.878; 0.997
11	6	~370	Cylindrical	LH	0.47	47.6	351	44.1	He	450	(6)	0.908; 1.033
11	9	~370	Cylindrical	LH	0.624	63.3	352	29.4	He	450	(6)	1.043; 1.187
11	10	~370	Cylindrical	LH	0.939	95.1	211	44.1	He	180	(6)	0.48; 0.527
11	11	~370	Cylindrical	LH	0.939	95.1	214	44.1	GH	180	(6)	1.267; 1.277
12	1	500	Cylindrical	LH	2.995	303.4	89	45.5	GH	300	(4), (17)	1.56
12	2	500	Cylindrical	LH	2.388	262.1	103	47.6	GH	520	(4), (17)	2.23
12	3	500	Cylindrical	LH	2.22	224.8	120	46.5	GH	300	(4), (17)	1.8
12	5	500	Cylindrical	LH	2.694	272.90	99	45.5	He	300	(4), (17)	1.72
13	?	461.5	Sphere	SLH	1.478	131	190	50	GH	520	(8)	2.568
13	?	461.5	Sphere	SLH	0.552	48.9	510	25	GH	620	(8)	10.34
13	?	461.5	Sphere	SLH	0.668	59.2	420	50	GH	620	(8)	5.973
14	2 of Ref. 33	210	Cylindrical	LH	1.062	106.6	93	161	GH	210		2.12
14	3 of Ref. 33	210	Cylindrical	LH	0.346	35	284	57	GH	170		3.88
14	8 of Ref. 33	210	Cylindrical	LH	1.161	116.6	90	159	He	161		2.14
14	10 of Ref. 33	210	Cylindrical	LH	0.311	31.6	309	40	He	148		5.1
15	4 - 11	600	Horizontal Cyl	LH	0.56	57	420	27.5	GH	480 - 549	(9)	1.2 - 1.25
15	3	600	Horizontal Cyl	LH	0.31	31	1220	35	GH	480 - 549	(9)	4.32
15	7	600	Horizontal Cyl	LH	1.56	157	340	115	GH	480 - 549	(9)	1.67
15	9	600	Horizontal Cyl	LH	2.48	250	560	115	GH	480 - 549	(9)	2.20
15	5	600	Horizontal Cyl	LH	2.53	256	450	65	GH	480 - 549	(9)	2.52
15	6	600	Horizontal Cyl	LH	0.84	85	410	65	GH	480 - 549	(9)	1.80
16		489	Sphere	LH	2	202	130	50	GH	500		~2.38
16		489	Sphere	LH	0.5	50.6	522	50	GH	500		~3.33
16		8604	Sphere	LH	10.3	1043	446	50	GH	500		~2.29
16		8604	Sphere	LH	4.33	438	1060	50	GH	500		~2.86
16		489	Sphere	LH	1.89	191	138	50	GH	540		~2.76
16		8604	Sphere	LH	10	1012	459	50	GH	600		~2.33
17	7	489	Sphere	LH	0.65	65.9	453.4	50	GH	481 - 517	(10)	~2.86
17	10	489	Sphere	LH	1.86	187.9	193.2	50	GH	481 - 517	(10)	~2.53

**Table 2 Selected Empirical Collapse Factor Data for Hydrogen Propellant Tanks (Continuation from Previous Page)**

Reference Citation	Test Run #	Tank Volume (gallons)	Tank Shape	Prop.	Propellant Expulsion				Pressurant Gas		Notes	Empirical Collapse Factor
					Mass Flow Rate (lb/sec)	Vol. Flow Rate (gpm)	Time (sec)	Tank Press. (psia)	Species	Inlet Temp. (deg R)		
17	12	489	Sphere	LH	0.77	77.5	393.2	50	GH	481 - 517	(10)	~3.03
17	14	489	Sphere	LH	0.92	92.9	337	50	GH	481 - 517	(10)	~2.94
17	15	489	Sphere	LH	1.32	133.9	249.7	50	GH	481 - 517	(10)	~2.70
17	83	489	Sphere	LH	0.67	67.5	428.8	50	GH	481 - 517	(10)	~3.20
17	84	489	Sphere	LH	0.98	98.8	307.6	50	GH	481 - 517	(10)	~2.73
17	85	489	Sphere	LH	1.91	193	174.4	50	GH	481 - 517	(10)	~2.58
18	4	8604	Sphere	LH	9.60	972	531.6	50	GH	302	(10)	1.85
18	7	8604	Sphere	LH	4.28	433	1119.3	50	GH	302	(10)	2.07
18	8	8604	Sphere	LH	4.66	472	1037.2	50	GH	303	(9), (10)	2.07
18	15	8604	Sphere	LH	10.07	1019	509.3	50	GH	540	(10)	2.60
19	5	1291	Oblate Spheroid	LH	0.60-0.65	66.3	2160	54.6	GH	491	(11), (15)	5.222
19	5 R	1291	Oblate Spheroid	LH	0.38-0.40	66.3	1680	54.7	GH	491	(12), (13)	5.333
19	6	1291	Oblate Spheroid	LH	0.60-0.65	40.8	2280	54.9	GH	491	(13), (15)	5.0
19	9	1291	Oblate Spheroid	LH	0.60-0.65	66.3	1620	55.0	GH	594	(14), (15)	4.933
20	506	1291	Oblate Spheroid	LH	~0.83	83.6	760	33.9	GH	529		2.46
20	507	1291	Oblate Spheroid	LH	~0.58	58.5	1086	44.3	GH	531		2.568
20	508	1291	Oblate Spheroid	LH	~0.32	32.2	1974	44	GH	533		2.58
20	509	1291	Oblate Spheroid	LH	~0.84	84.7	741	54.3	GH	535		2.85
20	510	1291	Oblate Spheroid	LH	~0.58	58.3	1089	54.9	GH	531		2.74
20	511	1291	Oblate Spheroid	LH	~0.32	32.1	1978	55.1	GH	526		2.86
21	?	489	Sphere	SLH	~0.55	52.3	505	35	He	540	(8)	3.788
21	?	489	Sphere	SLH	~1.26	120.0	220	35	He	540	(8)	3.178
21	?	489	Sphere	SLH	~0.54	51.8	510	35	He	250	(8)	2.100
21	?	489	Sphere	SLH	~1.38	132.0	200	35	He	250	(8)	1.591
21	?	489	Sphere	SLH	~0.58	55.0	480	35	He/GH	540	(2), (8)	6.655
21	?	489	Sphere	SLH	~1.32	125.7	210	35	He/GH	540	(2), (8)	3.727

- Notes:
- (1) Time includes ~12 sec. main ramp up of tank pressure; indicated flow rates are at main stage after this ramp up
  - (2) Pre-pressurized with helium followed by expulsion with hydrogen pressurant gas
  - (3) Propellant expulsion flow rates approximated by scaling of tank geometry drawings, given initial ullage height, liquid level change in tank with associated time span; Collapse Factor data also reported in Ref. 14
  - (4) Horizontal sloshing in tank at 0.5-Hz and 0.5-inch amplitude throughout expulsion
  - (5) Horizontal sloshing in tank at 0.5-Hz and 0.5-inch amplitude for last 85-seconds of expulsion
  - (6) Two collapse factors; first based on constant ullage gas temperature and pressure throughout expulsion; second based on saturated GH vapor in ullage at one atmosphere before tank pressurization
  - (7) Propellant mass flow rate data obtained from average LH propellant consumption of 5-each J-2 rocket engines on Saturn launch vehicle S-II stage from Ref. 9; tank pressure also obtained from this reference
  - (8) SLH is slush hydrogen, mixture of solid and liquid hydrogen
  - (9) Pressurant gas inlet temp. not reported; est. based on description of test apparatus and procedures
  - (10) Initial 30 to 56 sec. of the total time is tank pressurization and hold prior to propellant expulsion
  - (11) Submerged injection of pressurant gas, 21 min. tank pressurization, 15 min. CLH expulsion
  - (12) Submerged injection of pressurant gas, 13 min. tank pressurization, 15 min. CLH expulsion
  - (13) Submerged injection of pressurant gas, 13 min. tank pressurization, 25 min. CLH expulsion
  - (14) Submerged injection of pressurant gas, 12 min. tank pressurization, 15 min. CLH expulsion
  - (15) Initial 12- to 21-minutes of the total time is tank pressurization and hold prior to propellant expulsion
  - (16) Test runs are from unpublished report cited in Ref. 5
  - (17) Test run nos. are from another document cited in Ref. 12



## 1. Ullage Gas Region Vertical Temperature Gradients

Table 3 presents selected references where vertical ullage gas temperature distribution data were obtained from direct temperature measurements within the ullage gas region during tank pressurization and pressurized propellant expulsion processes. The propellant and pressurant gas species and other selected operating conditions are also presented in Table 3.

In a small portion of the cases presented in Table 3, propellant expulsions from the tank were not performed and tank pressurizations were accomplished by closing all valves connected to the tank and using the naturally

**Table 3. Selected References Containing Empirical Ullage Gas Region Vertical Temperature Distribution/Gradient Data**

Reference Citation	Test Number	Prop.	Press. Gas	Press. Gas Inlet Temp. (deg R)	Prop. Expul. Time (sec)	Ullage Gas Region Vertical Temp. Gradient (deg R)	
						Min.	Max.
4	8	LCH <sub>4</sub>	GCH <sub>4</sub>	400	231	?	174.6
4	6	LCH <sub>4</sub>	GCH <sub>4</sub>	400	633	?	176.4
4	11	LCH <sub>4</sub>	GCH <sub>4</sub>	600	234	?	369
4	37	LCH <sub>4</sub>	He	400	223	?	211
4	42	LCH <sub>4</sub>	He	600	224	?	380
4	63	LCH <sub>4</sub>	GH	400	219	?	193
4	68	LCH <sub>4</sub>	GH	600	222	?	398
10	3	LH	GH	300	120	?	218.5
10	5	LH	He	300	99	?	223.5
10	7	LH	GH	300	111	?	255.5
11	1	LH	He	450	217	342	405
11	3	LH	He	450	197	351	405
11	7	LH	He	450	375	405	405
11	11	LH	GH	180	214	149.4	193
12	1 (Fig. 5 of Ref.)	LH	GH	300	89	~223.5	~248.5
16	?	LH	GH	520	278	?	~460
16	?	LH	GH	520	278	?	~305
17	88	LH	GH	331	396	?	250
17	85	LH	GH	488	137	?	445
17	97	LH	GH	603	134	?	650
18	4	LH	GH	306	478	?	247
20	509	LH	GH	531	1110	245	423
20	510	LH	GH	529	741	?	405
20	511	LH	GH	526	1978	?	392
22	B-2	LH	N/A	N/A	N/A	80.1	126
23	(Fig. 4 of Ref.)	LOX	GOX	540	100	288	333
24	RT-3	LN	GN	~520	175	140	195
25	2.0-6	TPLH	GH	540	~980	193	238
25	2.0-8	TPLH	He/GH	144 and 540	~870	180	211
26	130-15	LOX	He	500 - 605	120	380	405
27	?	LH	N/A	N/A	14400	5.4	49.5
27	?	LH	N/A	N/A	14400	4.5	48.6
28	?	LH	GH	~525	130	?	~475
28	?	LH	GH	~525	130	?	~435
28	?	LH	GH	~525	130	?	~245
29	130-6	LOX	GOX	540	150	302	372
29	130-9	LOX	GOX	370	150	147	207
30	Ex. 1	LH	GH	488-525	90	?	428
30	Ex. 1	LH	GH	488-525	178	?	428
30	Ex. 1	LH	GH	488-525	320	?	428
30	Ex. 2	LH	GH	480-515	93	?	436
30	Ex. 3	LH	GH	375-520	284	?	450
30	Ex. 4	LH	GH	450-580	101	?	455
30	Ex. 5	LH	GH	395-273	95	?	208
30	Ex. 6	LH	GH	380-630	88	?	575
30	Ex. 7	LH	He	525-535	355	?	475
30	Ex. 8	LH	He	525-530	90	?	475
30	Ex. 9	LH	He	325-215	100	?	165
30	Ex. 10	LH	He	350-610	309	?	597
31	AS-203 (Saturn IB Launch 7/66)	LH	N/A	N/A	22,498	7	195

occurring heat transfer into the tank or externally supplied heat to vaporize cryogenic liquid propellant and heat all fluids inside the tank.

Virtually all of the cases presented in Table 3 indicate very large vertical temperature gradients ullage gas region. The differences between maximum and minimum temperatures in this region range from 150 R to 475 R.

In the majority of cases, the vertical temperature profiles in the ullage gas regions are more linear at the end of propellant expulsion than during initial tank pressurization and the start of propellant expulsion.

## 2. *Horizontal Temperature Gradients in Ullage Gas Region*

Although the data are extensive with regards to vertical temperature profiles and gradients in cryogenic propellant tank ullage gas regions, data are limited with regards to horizontal (or radial) temperature gradients. Table 4 contains selected data and includes the literature citations. For the majority of cases, tank wall temperatures are measured at the outside surfaces of the tank wall. While the data in Table 4 do show large temperature differences between the tank vertical centerline and the corresponding tank wall surface at or near the same elevation, there are no data showing the full horizontal temperature distribution from tank vertical centerline to tank wall. Also, for nearly all cases the large horizontal temperature gradients from tank vertical centerline to tank wall are confined to the upper sections of the ullage gas region near the elevations where pressurant gas enters the tank ullage.

Although not supported with data, many of the horizontal temperature gradients are likely to exist in a very thin boundary-layer region near the inner tank wall surface with little or no temperature variations outside this boundary layer. Also, for 20 of the 29 cases cited in Table 4, a moderate-to-significant portion of the horizontal temperature gradients could also be through the thickness of the tank walls since the tank wall temperatures are measured on the external wall surfaces. Although tank walls are thin, less than 1/2-inch thick, for cases shown on Table 4, expulsion times are also relatively short, on the order of 90 seconds to 400 seconds. These short exposure times of colder tank walls to the warmer ullage gas could result in large temperature gradients through the tank wall.

One study<sup>20</sup> not cited in Table 4 presents horizontal temperature uniformity data for various cryogenic propellant tank pressurization and propellant expulsion processes. For seven of the 14 tests in this study where the LH tank is pressurized with no propellant expulsion, predefined criteria for horizontal ullage gas temperature uniformity are satisfied. These criteria are also satisfied for four of the six LH propellant expulsion tests. For the remaining two LH expulsion tests and for one LH tank pressurization test without propellant expulsion, "approximate" horizontal ullage gas temperature uniformity is observed.

Other references<sup>7,16-18,23,26,28,30</sup> contain discussion about horizontal ullage gas temperature. In References 23 and 28, general statements that temperatures were found to have small variations in radial directions from the tank vertical axis are made, but no further data or information is presented. In References 7, 16, 17, 18, and 30, the tests include the use of horizontal temperature probe rakes at multiple, discrete elevations inside the test tanks.

## 3. *Multiple Species in Ullage Gas Region*

Although temperature distribution within the ullage gas region of a cryogenic propellant tank nearly always has the dominant effect on the distribution of ullage gas regional properties distribution that ultimately affects pressurant gas requirements, the mass fraction of constituent gases in a multi-component gas mixture within the ullage region can also have significant effects on the fluid property distribution in this region. Mixtures of two or more constituent gas species occur whenever pressurant gases are not the same species as the cryogenic propellant and when one or both of the following conditions exist:

- 1.) The cryogenic propellant tank is not completely filled with liquid cryogen, such that an ullage gas region exists, prior to the initial pressurization of the tank with externally supplied pressurant gas,
- 2.) Mass transfer of propellant species from the propellant region to the ullage gas region occurs at any time during initial tank pressurization or pressurized propellant expulsion processes.

For virtually all cases, only one or two pressurant gas species are used for cryogenic propellant tank pressurization and pressurized propellant expulsion processes. When two pressurant gas species are used, one of the two species is generally the same species as the cryogenic propellant. Therefore, for nearly all cases and for purposes of this study, the ullage gas region is occupied by either a single gas species or a two-component (binary) gas mixture.

**Table 4. Selected Empirical Ullage Gas and Adjacent Tank Wall Temperature Data for Approximations of Ullage Gas Region Horizontal Temperature Gradients**

Reference Citation	Test Number	Prop.	Press. Gas	Press. Gas Inlet Temp. (deg R)	Expul. Time (sec)	Horizontal Temperature Gradient, Tank Vertical Centerline to Tank Wall (deg R)	
						Minimum	Maximum
4	8	LCH <sub>4</sub>	GCH <sub>4</sub>	400	231	0	117
4	6	LCH <sub>4</sub>	GCH <sub>4</sub>	400	633	0	80
4	11	LCH <sub>4</sub>	GCH <sub>4</sub>	600	234	0	281
4	37	LCH <sub>4</sub>	He	400	223	0	97
4	42	LCH <sub>4</sub>	He	600	224	0	180
4	63	LCH <sub>4</sub>	GH	400	219	2	99
4	68	LCH <sub>4</sub>	GH	600	222	0	225
10	3	LH	GH	300	120	0	~63
10	4	LH	GH	300	87	4.5	~72
10	5	LH	He	300	99	0.5	51
10	6	LH	He	300	95	26	95
10	7	LH	GH	300	111	9	71
11	4	LH	He	450	205	9	107
11	7	LH	He	450	375	0	130
11	9	LH	He	450	352	-5	126
11	11	LH	He	180	214	0	59
11	19	LN	GN	?	N/A	0	107
12	1	LH	GH	300	89	0	99
17	88	LH	He	331	396	2	100
17	85	LH	He	488	137	19	282
17	87	LH	He	603	134	0	540
18	4	LH	He	306	478	2	55
27	?	LH	N/A	N/A	N/A	1	29
30	Ex. 1	LH	GH	488 - 520	350	15	220
30	Ex. 4	LH	GH	450 - 580	101	0	300
30	Ex. 6	LH	GH	385 - 630	88	0	415
30	Ex. 8	LH	He	524 - 530	90	~20	270

Experimental data or the reduction/conversion of this data from References 4, 17, 18, 24, 32, 33, and 34 confirm that mass transfer of propellant species into the ullage gas region does often occur during cryogenic propellant tank pressurization and pressurized propellant expulsion processes.

## B. Propellant Region Properties Distribution

Although not as significant as ullage gas region property distributions, pressurant gas requirements can be affected by the distribution of properties within the cryogenic propellant region of a pressurized tank. In contrast to ullage gas property gradients and distribution, which are likely to have direct and significant effects on collapse factors, the propellant property gradients and distribution are likely to have indirect and less significant effects. In this region, as with the ullage gas region, fluid temperature distribution has the predominant effect on property distributions.

In the propellant region, fluid densities are generally greater, on the order of three times to one thousand times greater depending upon tank pressure and cryogenic propellant species, which means that vertical pressure gradients are much larger than those in the ullage gas region. However, the other fluid properties (including density, thermal conductivity, specific heat, and viscosity) which affect heat and mass transfer processes (and which ultimately affect pressurant gas requirements), are not significantly affected by the spatial pressure distribution within the propellant region. Examination of data from Ref. 35 over a wide range of tank pressures and cryogenic propellant temperatures was performed as part of this study. The results of this examination substantiate the minor effects of pressure variations on fluid properties in the ullage gas and propellant regions. Pressures in these regions vary by less than 50-psia for nitrogen and oxygen and less than 0.2-psia for hydrogen with the typical sizes and geometries of cryogenic tanks.

However, the possible variations in temperature within the cryogenic propellant region does have a much more significant effect on the critical fluid properties affecting heat and mass transfer within and across the boundaries of the cryogenic propellant region.

### 1. Propellant Region Vertical Temperature Distribution

Table 5 provides a summary of selected references where empirical vertical temperature gradient data is provided for cryogenic propellant regions inside various tanks.

**Table 5. References with Empirical Propellant Vertical Temperature Gradient/Profile Data**

Reference Citation	Test Number	Prop.	Press. Gas	Propellant Height (ft.)		Press. Hold or Expul. Time (sec.)	Tank Press. (psia)
				Minimum	Maximum		
4	9	LCH <sub>3</sub>	GCH <sub>4</sub>	~-0.85	~-4.15	638	48.6
4	10	LCH <sub>3</sub>	GCH <sub>4</sub>	~-0.85	~-4.15	410	48.9
4	11	LCH <sub>3</sub>	GCH <sub>4</sub>	~-0.85	~-4.15	234	49.2
4	97	LCH <sub>3</sub>	GN	~-0.85	~-4.15	568	49.5
4	98	LCH <sub>3</sub>	GN	~-0.85	~-4.15	232	49.5
10	3	LH	GH	1	7.25	120	46.5
10	4	LH	GH	0.08	6.75	87	46.6
12	2	LH	GH	<0.50	7.46	103	47.6
12	5	LH	He	<0.50	7.51	99	45.5
12	6	LH	GH/He	<0.50	7.63	95	47.0
12	7	LH	GH	<0.50	7.33	111	45.0
12	10	LH	GH	<0.50	7.39	105	45.5
27	?	LH	N/A	4.59	4.59	14,400	14.7 - 18.4
27	?	LH	N/A	4.59	4.59	43,200	14.7 - 27.0
36	3L/min	Water	*	1.31	3.11	840	~14.7
36	15L/min	Water	*	1.31	3.11	180	~14.7
37	2	LN	N/A	3.17	3.17	60	39.7
37	2	LN	N/A	3.17	3.17	360	29.7
37	3	LN	N/A	3.17	3.17	60	29.7
37	3	LN	N/A	3.17	3.17	360	29.7
38	4	LH	He	13.17	13.17	119	18.7-32.7
38	Fig. 8	LH	GH	4.75	4.75	100	?
38	Fig. 8	LH	GH	4.75	4.75	600	?
39	13	LN	GN	1.98	1.98	7200	450
40	6.5L/min	Water	*	5.25	6.56	1500	~14.7
40	9L/min	Water	*	5.25	6.56	1500	~14.7
41	B-2	LH	N/A	6.02	6.02	40	16.5 - 17.4
41	B-2	LH	N/A	6.02	6.02	152	16.5 - 19.5
42	?	LH	N/A	3.75	8.52	20,700	19.15
43	?	LH	N/A	18.47	18.47	136,800	18.7 - 39.1
44	17	LH	N/A	3.91	3.91	120	~27
44	19	LH	N/A	1.38	1.38	400	~31.2
44	40	LN	N/A	3.97	3.97	160	~18.0
44	38	LN	N/A	1.27	1.27	700	~18.9
45	1	LH	GH	2.5	2.5	600	54.7
45	3	LH	GH	2.5	2.5	720	22.7
46	?	LH	GH	?	?	600	14.7 - 55
47	A-3	LH	GH	4.19	4.19	900	125 - 160
47	B-1	LH	GH	3.98	3.98	104,400	15.5 - 24.7
48	?	LH	N/A	2.36	2.36	600	14.7 - 73.5
48	?	LH	N/A	2.21	2.21	600	14.7 - 73.5
48	?	LH	N/A	2.30	2.30	600	14.7 - 73.5
48	?	LH	N/A	2.14	2.14	600	14.7 - 73.5
49	?	LH	N/A	6.50	6.50	120	?
49	?	LH	N/A	6.50	6.50	300	?

Cryogenic propellant region vertical temperature gradients are generally on the order of 5 R to 30 R. Also, the majority of data from references cited in Table 5 show that the major portion of the vertical temperature gradient has a vertical height that does not exceed 2% to 20% of the total propellant region height at the start of propellant expulsion from the tank or when the tank is 80% to 90% full of liquid propellant. For larger tanks, this major portion of the vertical temperature gradient extends from three inches to three feet below the interface between propellant and ullage gas; while for smaller tanks this depth below this interface is nominally 6-inches or less. Below these depths, where the major temperature gradient exists, the cryogenic propellant temperature is nearly uniform within 1 R.

Three studies<sup>12,38,44</sup> present cases where larger vertical temperature gradients occur through more than 20% of the maximum or initial height of the propellant region. However, for the cases where this phenomenon was observed, high heat fluxes were applied by enhanced heating of tank walls or liquid propellant sloshing was induced by horizontal tank oscillatory motions. However, even for these cases, vertical temperature gradients through the entire cryogenic propellant region are usually less than 5 R and never exceed 10 R.

Approximately half of the cases presented in Table 5 are those where a tank is partially filled with cryogenic liquid propellant and no propellant expulsion from the tank is occurring. In most of these cases, tank pressurization is provided by heating and boil-off of liquid propellant through normal heat leak or enhanced heat input into the tank. A few cases involve the use of externally supplied pressurant gas for initial tank pressurization.

References 36 and 40 are cases where tanks are completely filled with water with a region of colder water below a region of warmer water where heated water is supplied into the top of the tank as the cooler water is discharged from the bottom of the tank. These references are presented because they illustrate that most of the temperature gradient for the lower region of cooler water is confined to a small upper portion of this region, even when the upper boundary of this region is in contact with liquid water at higher temperature and having thermal conductivity that is much higher than that of gases.

In addition to references cited in Table 5, a number of other studies<sup>32,48,50-53</sup> present or discuss similar results with liquid and cold supercritical cryogenic fluids in tanks

## 2. *Propellant Region Horizontal Temperature Distribution*

Empirical data from a number of the cited references in Table 4 indicate zero or extremely small horizontal temperature gradients in the cryogenic propellant region. A large number of graphical plots in these references illustrate both the tank wall and ullage gas temperatures approaching the temperature of the bulk cryogenic propellant, within 0 R to 20 R, when traversing from the top of the tank down to the interface between ullage gas and cryogenic propellant.

For cases where the horizontal temperature gradient in the propellant region can have temperature variations as high as 10 R to 40 R, there are data from studies that indicate that virtually all of this gradient exists in a very thin thermal boundary layer adjacent to the tank walls.

## 3. *Multiple Species in Propellant Region*

For the cases where the pressurant gas is not the same species as the cryogenic propellant, the pressurant gas species can dissolve or condense into the cryogenic propellant region. This phenomenon has the net effect of making a portion of the fluid in the propellant region a mixture of pressurant gas and propellant species where both can be liquids, supercritical fluids, or solution of vapor dissolved within the liquid propellant. When this condition occurs, there is also a variation of fluid properties within the cryogenic propellant region caused by mass fraction variations of the constituent fluid species. Mass fraction of pressurant gas species is likely to be highest at the ullage-gas-to-propellant interface, and the mass fraction generally decreases as the vertical depth below this interface increases.

Although actual empirical data are very limited, a number of studies<sup>4,10,17,18,34,54-56</sup> do report findings where pressurant gas species is present within the cryogenic propellant where the cryogenic propellant and pressurant gas are different species.

### C. Tank Wall Temperature Distribution

The distributions of temperatures through the tank walls have not been directly measured for cryogenic tanks. A number of studies include measurement of tank wall temperatures at discrete locations on the outer or inner wall surface in addition to discrete temperature measurements within the propellant and ullage gas regions (usually near the tank's vertical axis centerline). Table 4, presented earlier in this chapter, cites most of the studies where this was done. Two studies<sup>34,57</sup> also include empirical tank wall temperature data.

The predominant simplifying assumption with regards to analytical modeling of heat and mass transfer processes in cryogenic propellant tanks is that of a negligibly small temperature gradient through the tank wall thickness normal to the inner wall local tangent plane. Virtually all of the data from prior studies<sup>4,11,17,18,27,30,34</sup> indicate that either this is a valid assumption or that the resultant errors in determining pressurant gas requirements are negligible or acceptably small.

The studies cited above also compare analytically predicted tank wall temperatures with experimentally measured tank wall temperatures. References 4, 11, and 17 provide experimental outer wall temperature data where measured temperatures are generally 5 R to 20 R colder than analytically computed temperatures, except for a few cases in Ref. 11 where experimentally measured temperatures were 45 R colder. Two studies<sup>18,34</sup> report experimentally measured tank outer wall temperatures to be 0 R to 10 R warmer than analytically computed temperatures. With the exception of a few isolated cases, data from all studies indicate that temperature gradients through the tank wall thickness have temperature differences of less than 20 R between inner and outer surfaces of the tank walls. This holds true even in a study<sup>27</sup> where external heat fluxes were applied to the outer tank wall surface for one to 14 hour durations.

In addition to the temperature distributions through the tank wall normal to the plane tangent to each local inner wall surface (through thickness of the wall), the temperature distribution parallel to the tank wall inner and outer surfaces needs to be considered. Many of the studies cited in Table 4 also present data confirming that the outer and inner tank wall surface temperature varies significantly with respect to vertical position from the top of a tank downward to the interface between ullage gas and cryogenic propellant. The general trends show the wall surface temperature decreasing in either a near-linear or highly non-linear fashion when traversing from top of tank downward to the vertical position of the ullage-gas-to-propellant interface. These data indicate that the tank wall surfaces have a much colder temperature than the ullage gas at the same corresponding vertical position where the range of typical temperature differences are shown in Table 4.

For all of the cited references in Table 4 where vertical ullage gas and tank wall temperature profile are shown, the general trend shows that the difference between ullage gas temperature and tank wall surface temperature decreases when traversing from the top of the tank or from the elevation(s) where pressurant gas enters the tank ullage downward to the aforementioned interface. When approaching this interface from above the ullage gas temperature and tank wall temperature both converge to nearly the same temperature that is nearly equal to, within 10 R and usually within 1 R to 2 R of, the bulk cryogenic propellant temperature.

Regarding tank wall temperature profiles in the vicinity of the interface between ullage gas and cryogenic propellant regions, the empirical data all indicate that heat conduction through the tank wall parallel to the inner tank wall surface tends to "smooth out" or eliminate the occurrence of any abrupt temperature changes through the tank wall.

The phenomena described in the above two paragraphs are supported or confirmed with data presented various references<sup>4,11,17,18,27,30,34,51</sup>. Two studies<sup>27,51</sup> indicate that these phenomena exist also when tank outer wall surfaces are heated with a constant heat flux.

No empirical tank wall temperature data were found in the research of studies for cases where tank pressures were near critical or supercritical nor for cases with heavy walled cryogenic propellant tanks with wall thicknesses above 1/2-inch.

## D. Effects of Mass Transfer on Pressurant Gas Requirements

Most of the studies cited in the "Multiple Species in Ullage Gas Region" and "Multiple Species in Propellant Region" subsections acknowledge the potential for mass transfer processes between ullage gas and cryogenic propellant regions to have significant effects on required mass transfer of pressurant gas into the tank ullage. A number of the studies also conclude that this mass transfer can have effects that either increase or decrease the requirements depending on a number of parameters and operating conditions. However, there are also a number of prior studies that report very accurate predictions of requirements from analytical models when treating mass transfer between ullage gas and cryogenic propellant as negligible. The data from Ref. 30 is one example. On the other hand, studies where enhanced mass transfer between ullage gas and cryogenic propellant is known to have occurred (usually due to induced propellant sloshing) state significant increases in collapse factors over those where no propellant sloshing occurred. The data of Ref. 4 are examples indicating this occurrence. For other selected studies, the results are mixed where enhanced mass transfer due to propellant sloshing increases collapse factors significantly in some cases and has minor or negligible effects in other cases. The data of Ref. 10 as reported by Ref. 14 are examples where mixed results occurred.

Perhaps the studies that most clearly demonstrate the significance of mass transfer effects on collapse factors are in References 4 and 6. In the latter reference, the second test series has empirical collapse factors that are nominally two to three times lower than collapse factors from similar and corresponding tests from the first test series. The cause of this very significant collapse factor reduction is greatly enhanced vaporization of the LOX propellant and mass transfer of this vaporized propellant into the tank ullage gas region when helium gas is bubbled up through this propellant. On the other hand, Ref. 4 reports very high collapse factors due to significant mass transfer of GN pressurant into LCH<sub>4</sub> propellant where 60 to 75% of the pressurant gas supplied to the tanks is dissolved into the propellant. Further analyses and tests presented in this study indicate the density of LCH<sub>4</sub> with dissolved GN increases as the concentration of GN increases which enhanced the buoyancy driven mixing of GN into a large portion of the propellant region. The use of GN pressurant gas was subsequently rejected as a cost savings option to replace helium.

The net result from the data in prior studies is that there is no consistent trend regarding the magnitude and direction of mass transfer across the interface between ullage gas and cryogenic propellant regions. The same is likely to be true for mass transfer of propellant species within the ullage gas region when pressurant gas and cryogenic propellant are different species, but there is insufficient empirical data to substantiate this. There is also no consistent trend or level of influence with regards to how this mass transfer ultimately affects collapse factors.

With respect to cryogenic propellant tanks operating at supercritical and high subcritical pressures, no empirical data for mass transfer across the ullage-gas-to-propellant interface have been found. From the studies researched, the effects of this mass transfer on collapse factors have not been evaluated in depth for the higher tank operating pressure conditions.

## E. Pressurant Gas Entry Effects

The controlling-parameter that generally has one of the strongest influences on pressurant gas requirements and associated collapse factors in cryogenic propellant tanks is fluid flow conditions within and across volume boundaries in the tank. These conditions are predominantly influenced by pressurant gas flow velocity vectors at the point(s) of entry into the tank ullage gas region. Extensive empirical data indicate that these velocity vectors can yield two to six fold increases in convection heat transfer between the ullage gas and tank walls as well as between the ullage gas and cryogenic propellant. Additionally, these velocity vectors can provide forced mixing within the ullage gas region to create more uniform temperatures within most, or all, of the upper ullage gas region which can have either a beneficial effect in reducing ullage collapse or a detrimental effect by increasing this collapse. Pressurant gas inlet velocity vectors directed downward into the tank ullage and along tank walls can cause moderate to high levels of forced mixing between the ullage gas and cryogenic propellant.

Eleven studies<sup>12,19,58-66</sup> provide data, observed cases, or indications where enhanced mixing between ullage gas and propellant increases pressurant gas mass transfer requirements and associated collapse factors, often by factors of two or three.

A number of other studies<sup>16,45,61, 67</sup> support the concept of reducing ullage collapse by prevention of forced mixing between ullage gas and cryogenic propellant, but they report or conclude that enhanced mixing within the ullage gas region, rather than keeping this region stratified, also serves to reduce collapse factors.

In addition to the studies described above for cryogenic tank pressurization followed by pressurized propellant expulsion processes, there are a number of studies where methods to intentionally increase ullage gas collapse are employed to reduce or eliminate the need to vent (and lose) ullage gas from a cryogenic fluid tank during long term storage. The main end-use applications for these studies are onboard spacecraft cryogenic liquid tank systems to reduce quantities of lost and wasted fluids as much as possible. All of these studies provide strong indications that enhanced heat and mass transfer between ullage gas and cryogenic liquid propellant does cause significant collapsing (with associated pressure reduction) of the ullage gas. A number of studies<sup>68-78</sup> provides empirical data showing ullage gas collapse through this enhanced heat and mass transfer.

In summary, the effects of pressurant gas entry velocities and conditions into cryogenic propellant tanks on collapse factors are not always consistent. While some data indicates that enhanced mixing within the ullage gas region to attain more uniform properties within this region reduces collapse factors, other data indicates that maintaining a thermally stratified ullage gas region lowers collapse factors.

With the exception of cases where helium pressurant gas is bubbled up through LOX and LCH<sub>4</sub> propellant at low (50-psia nominal) subcritical pressures, enhanced mixing between ullage gases and cryogenic propellants results in increased pressurant gas requirements and associated collapse factors. The requirements tend to increase when the effects of ullage gas temperature reduction dominate over the effects of mass addition to the ullage gas region when vaporized propellant transfers to this region. This dominant effect appears to be the case most of the time. The exceptions appear to be cases where the effects of added propellant mass dominate.

A consistent trend observed in all studies is the reduction of mass transfer across the ullage-gas-to-cryogenic-propellant interface to very low or negligible levels when this interface is not disturbed with enhanced mixing of fluids across this interface and when the molecular weight of the pressurant gas species is less than that of the propellant species or helium pressurant gas is used.

Another consistent trend supported by all studies cited in this section where ullage-gas-to-tank-wall heat transfer is evaluated indicates the reduction of this heat transfer is a primary method to reduce ullage collapse and the resulting pressurant gas requirements.

As with much of the empirical data, there are no data regarding pressurant gas entry effects on its mass transfer and flow rate requirements for cryogenic propellant tanks operating at supercritical and high subcritical pressures.

#### **IV. Analytical Methods and Models to Predict Collapse Factor**

A wide variety of analytical models and computational techniques have been devised to predict or to provide reliable and practical methods in determining collapse factors and the associated mass and mass flow rate requirements of cryogenic propellant tank pressurant gases. Initial work, starting in the late 1950's, has been focused on analytical methods that would consistently and reliably predict pressurant gas requirements that were sufficiently higher than actual requirements such that a conservative safety margin was always provided for design of pressurant gas subsystems. Through the 1960's as launch vehicle liquid propulsion systems were being developed for the space program and their cryogenic propellant tanks grew in size, the prediction of pressurant gas requirements with reduced margins of conservatism and errors grew in importance. For the larger flight vehicles weight reductions including those of the cryogenic liquid propellant tank pressurant gases and their supply subsystems, was of premium importance. This resulted in the development of elaborate computer based programs or empirically based computation methods to determine collapse factors.

In the late 1980's and early 1990's analytical work was performed to predict collapse factors more accurately for supercritical tank pressure applications. The work presented in References 79 and 80, with the reduction of



empirical data from Ref. 8, are the major efforts in this area. From these efforts, predicted collapse factors ranged nominally from 1.05 to 1.40 and empirically obtained collapse factors ranged from 1.42 to 4.10 with the higher values occurring at the start of propellant expulsion reducing to cumulative collapse factors between 1.05 and 1.60 at the end of this expulsion process.

In this article, the presented studies are mostly limited to cases where cryogenic propellant tanks are on the Earth's surface and where the model can be readily adapted to tanks on accelerating flight vehicles. However, selected studies performed for micro-gravity conditions are also mentioned where they provide selected characteristics and insights.

### **A. "Saturation Rule"**

For the earlier pressurized cryogenic liquid tank expulsion and transfer studies performed in the late 1950's and early 1960's, analytical techniques using the "Saturation Rule" have been employed to predict or provide a conservative estimate of pressurant gas requirements. The "Saturation Rule" is based on the assumption that the ullage gas is always at a density corresponding to the saturation temperature of the cryogenic propellant and the tank pressure. If the ullage gas is the same species as the propellant, then the ullage gas is assumed to be a saturated vapor. The initial and final ullage gas volumes and densities are then used to compute the net addition of mass to the ullage region.

Use of the "Saturation Rule" is presented in References 55, 62, and 81 for LN and LOX expulsions with nitrogen and oxygen pressurant gases. When comparing the saturation rule results with test data, the analysis results had errors ranging from 16.3% under-predicted to 10.0% over-predicted in Ref. 55.

In Ref. 62 use of the "Saturation Rule" is combined with evaluation of ullage gas condensation along cylindrical tank walls where the tank was immersed in a bath of LN at near atmospheric pressure (LN bath temperature near  $-320\text{ F} \cong 140\text{ R}$ ). When comparisons of empirical data to analytically predicted data are made in this reference, the predicted pressurant gas requirements are consistently higher than those from empirical data with errors within 11% for most of the time duration of each liquid cryogen expulsion process. However, the predicted pressurant gas mass flow rate data near the start of cryogenic liquid expulsions are nearly two times higher than data from experimental tests.

### **B. Modifications and Enhancements to the "Saturation Rule"**

Subsequent studies<sup>15,24</sup> found that analytical results using the "Saturation Rule" were excessively conservative (predicted pressurant gas requirements were four to ten times higher than those from actual tests) or resulted in physically impossible conditions for LH expulsions using hydrogen pressurant gas. Ref. 15 presents a revised technique using the "Worst Case Rule" which is based on the following assumptions:

- 1.) The tank is completely full of liquid cryogen at the start of expulsion (0% initial ullage gas volume),
- 2.) The pressurant gas exits the supply source and enters the tank at constant inlet enthalpy,
- 3.) The tank is at constant and uniform internal pressure,
- 4.) All pressurant gas that enters the tank displaces all of the liquid cryogen initially in the tank,
- 5.) All pressurant gas in the tank at the end of liquid cryogen expulsion is in the saturated vapor state.

Ref. 24 presents an alternative analytical method to the methods using the "Saturation Rule," although this method involves more steps and increased complexity as compared to that of Ref. 15. The method in the former reference is called the "Equivalent Mass Model."

Results obtained from use of the "Equivalent Mass Model" show 10.0% under-prediction to 12.8% over-prediction of pressurant gas required as compared to data. The "Equivalent Mass Model" proved to yield more accurate pressurant gas requirement results than both the "Saturation Rule" and "Worst Case Rule" analytical methods, but the computation processes are more complex and involved. Additionally the "Equivalent Mass Model" provides good comparisons with empirical data for a wide range of cryogenic liquid tank geometries and sizes from 3 to 28,000 gallons.

### C. Semi-Empirical Curve-fit Models

After the development of the "Equivalent Mass Model," semi-empirical models were developed, tested, and used for ground-based tank systems. These models were utilized for a large variety of tank sizes, diameter-to-height ratios, and combinations of liquid cryogen propellant and pressurant gases. Efforts were made to derive a single equation or a series of simple equations, that included a set of empirically-derived constants, where collapse factors and the associated pressurant gas requirements were computed explicitly. The equations all used various ullage gas, incoming pressurant gas, and tank wall material properties, tank geometric data, and either known heat transfer rates or thermal boundary-layer film temperature gradients with user input or computed convection heat transfer coefficients. The main purpose for development of the semi-empirical curve-fit models was to provide methods that enabled sufficiently accurate, with error less than 10% to 15%, computation of collapse factors and pressurant gas requirements without having to rely on the large and expensive mainframe computers that were needed in the 1960's for running the high fidelity and more complex computer program analysis tools used to predict collapse factors at that time.

Another semi-empirical computation method is presented in Ref. 54 in which six simultaneous equations are solved numerically by an iterative procedure. The net result is a computed final mean ullage gas temperature used to determine final mean ullage gas density and total mass. The collapse factors can then be computed. Errors of predictions for final mean ullage gas region temperatures are as large as 52 %.

Two studies<sup>5,57</sup> present a single semi-empirical correlation to directly compute cumulative collapse factors and required total mass of pressurant gas at the end of propellant expulsion processes. Errors of collapse factors predicted by the correlation when compared to those obtained empirically are all less than 12% with most falling between 5% and 6%. Also, the majority of results show that the correlation errs on the conservative side; i.e., the correlation predicts collapse factors higher than actual collapse factors from tests for most cases.

Later work presented in one study<sup>82</sup> provides enhancements to the collapse factor correlation described above. These enhancements include:

- 1.) Addition of new correlations to adjust parameters for cases where initial ullage gas volume is less than 20% of total tank volume,
- 2.) Addition of correlations to adjust parameters for cases where a large residual propellant volume remains in the tank at the end of propellant expulsion,
- 3.) Addition of a new correlation to compute an improved equivalent tank wall thickness and specific heat capacity for cases when the tank has highly non-uniform wall thicknesses including heavy walled nozzles and flange connections as well as accessory hardware inside the tank volume;
- 4.) Improved correlation to compute equivalent tank diameter, based on vertical cylindrical tanks geometries, for spherical and ellipsoidal tanks,
- 5.) Addition of revised and improved empirical constants for LH propellant expulsions.

Additionally, the study presented in Ref. 82 investigated the effects of mass transfer between cryogenic liquid propellant and ullage gas. The study concluded that evaporated propellant into the ullage gas region must be less than 26% of the total mass of pressurant gas supplied to the tank for the collapse factor correlation to be valid. The author also concludes that no more than 19% of the pressurant gas supplied to the tank ullage can condense into the propellant region to maintain validity of the collapse factor correlation.

An alternate and more comprehensive correlation is presented in Ref. 29 where final mean ullage gas temperature, at the end of cryogenic propellant expulsion, is computed by use of 19 fluid property, tank wall property, tank geometry, and pressurant gas inlet properties, and pressurant gas inlet flow condition variables.

The information presented in Ref. 83 is nearly identical to that of Ref. 29, but the former study contains added discussion about the computation of equivalent tank radius for non-cylindrical tanks. No comparisons between analytically computed and empirically obtained data are presented in either of these references.

## D. Upper and Lower Bound Analyses

More recent work performed in the middle 1980's through the early 1990's include upper and lower bound analyses in order to predict more realistic maximum and minimum possible mass requirements for pressurant gas in the expulsion of cryogenic propellants from tanks. A major focus of the upper and lower bound analyses is the ability to evaluate pressurant gas requirements for tanks operating at supercritical pressures.

The study presented in Ref. 15 can be classified as the original early version of an upper and lower bound analysis method. Subsequent works<sup>66,84-86</sup> provide analytical methods for determining upper and lower bounds of pressurant gas requirements.

The upper- and lower-bound analytical techniques have been shown to be consistently reliable in providing the possible ranges of cumulative collapse factors. However, the ranges are quite wide and the actual collapse factors and associated pressurant gas requirements are often well below upper-bound values even though the more recent studies have brought the upper bounds to more realistic and less conservative values.

## E. Lumped Mass Fluid Region Models

In parallel to development and use of the modeling methods described in the previous subsections of this chapter, models using numerical techniques to model intra-tank heat and mass transfer processes and requiring iterative computation methods have also been developed. When developed and utilized in the 1960's these models were in the form of computer programs. These computer programs involve the solution to two or more complex simultaneous equations where each contains and utilizes a number of dependent variables and where numerical techniques and multiple iteration routines are needed to arrive at converged solutions. The dependent variables mainly include selected thermal and transport properties of ullage gas and incoming pressurant gas, a limited number of cryogenic (liquid) propellant properties, selected tank wall geometric parameters, and selected tank wall material properties.

Table 6 provides a summation of data and selected details for the Lumped-Mass Fluid Region (LMFR) models researched for this study. Included in this table are general descriptions of the heat and mass transfer computation methods used at regional boundaries and the comparison of analytical model results with empirical results where the actual test conditions and parameters correspond to those modeled analytically.

With the exception of two studies<sup>79,80</sup> the tank wall is assumed to have a negligible temperature gradient through the thickness of the tank wall.

To account for non-uniform temperatures through thick tank walls, Ref. 80 models the inner 70% of the tank wall thickness to be uniformly heated by ullage gas while the remaining 30% of wall thickness is thermally isolated from the heated wall.

The model presented in Ref. 79 utilizes an explicit finite-difference technique from Ref. 87 to map the tank wall temperature distribution through the tank wall thickness at discrete time steps. The explicit finite-difference method is used because the thermal properties of cryogenic tank wall materials vary very widely and in a highly non-linear fashion with respect to temperature in the cryogenic temperature regimes.

Regarding vertical tank wall temperature distributions or the vertical component of the tank wall temperature profile parallel to the tank wall inner surface, the analytical models presented in references cited in Table 6 each employ one of two methods. The simpler method treats the entire section of tank wall in contact with ullage gas at each discrete time step as a lumped mass having a uniform temperature, or in the case of Ref. 79 a uniform temperature profile through the tank wall thickness.

**Table 6 Summary Data for Lumped Mass Fluid Region (LMFR) Models**

Reference Citation	Heat Transfer				Mass Transfer	Model Errors Compared to Empirical Data
	Ullage Gas to Wall	Propellant to Wall	Ullage Gas to Propellant	External Tank Wall	Ullage Gas to Propellant	
12	NLC, Correlation for Conv. H.T. Coeff. not provided	Based on H.T. from wall boiling liquid propellant	Not Discussed	NLC, Correlation for Conv. H.T. Coeff. not shown	Not Discussed	Range: -9.6 to 7.8%; Mean: 1.11%; Std. Dev. 5.0%; 10 Tests Compared
14	NLC, NC, Note 7	Assumed Negligible	Assumed Negligible	Not Discussed	Assumed No Mass Transfer	Range: -10.4 to 18.5%; Mean: 0.65%; Std. Dev. 7.74%; 18 Tests Compared
33	NLC, NC, Note 9	Assumed Negligible	Not Modeled	Modeled as Adiabatic	Determined from Empirical Data	Range: -9.0 to 8.4%; Mean: 0.34%; Std. Dev. 4.57%; 12 Tests Compared
79	NLC, NC, VP & HP [Ref. 87 Correlations]	NLC, NC, VP & HP [Ref. 87 Correlations]	NLC, NC, HPCSU [Ref. 87 Correlations]	Modeled as Adiabatic	Assumed Negligible	Pressurant gas supply bottle press. And temp. show < 1 K and <0.5 MPa error for part of Test 74 on E-8 Test Stand
80	NLC, NC & FC, Notes 3 and 5 [Ref. 34 Correlations]	Assumed Negligible	NLC, NC & FC, Notes 3 and 6 [Ref. 34 Correlations]	Modeled as Adiabatic, Note 5	None, equivalent mass transfer modeled by added H.T., Note 6	No comparisons presented; model predicts Collapse Factor of 1.20 to 1.24
88	Notes 1 and 3	Note 2	Note 4	Note 1	Note 1	Range: -9.3 to 13.1%; Mean: 2.75%; Std. Dev. 5.74%; 11 Tests Compared
89	NLC, NC	NLC, NC	Not Discussed	Not Discussed	Not Discussed	~10 to 12% estimated from UG Press. & Temp. data
90	NLC, NC, HPCSD	EC	NLC, NC, HPCSU	Not Discussed	Not Discussed	~18 to 30% based on comparison with model data in Epstein and Anderson (1968)
91	NLC, NC, Note 7	Assumed Negligible	NLC, NC, HPCSU [from Ref. 92]	Not Discussed	(1) and (2)	-14.1, 4.7, -1.8, 0% for GH over LH; -2.5, -8.7, 6.7, -2.5% for GHe over LH
92	NLC, NC, VP & FC	NLC, NC, VP & HP, FC	NLC, NC, HPCSU	NLC, FC & Radiation	(1), (6), and Note 8	No Comparisons Presented

Key: NLC = Newton's Law of Cooling  
 NC = Natural (Free) Convection  
 FC = Forced Convection  
 HP = Horizontal Plate (Natural Convection Correlations)  
 HPCSD = Horizontal Plate (Natural Convection Correlations), Cold Side Down  
 HPCSU = Horizontal Plate (Natural Convection Correlations), Cold Side Up  
 VP = Vertical Plate (Natural Convection Correlations)  
 EC = Equivalent Conduction; thermal conductivity and slope of temperature gradient across finite segment/element at boundary  
 (1) = First Mass Transfer Computation Technique, from "Mass Transfer Correlations" section of Chapter II of Ref. 3  
 (2) = Second Mass Transfer Computation Technique, from "Mass Transfer Correlations" section of Chapter II of Ref. 3  
 (6) = Sixth Mass Transfer Computation Technique, from "Mass Transfer Correlations" section of Chapter II of Ref. 3

- Notes:
1. An energy balance equation using propellant, mean ullage gas, entering pressurant gas, and tank wall temperatures; temperature differentials; and empirically determined coefficients is used to calculate rate of change of ullage gas temperature at discrete time steps.
  2. A condensation or evaporation energy balance equation, whichever has highest magnitude, using propellant, mean ullage gas, and tank wall temperatures; temperature differentials; and empirically determined coefficients is used to calculate rate of change of liquid propellant temperature at discrete time steps.
  3. Ullage gas is divided into two regions; the lower region contains only the initial mass of ullage gas prior to entry of pressurant gas and the upper region contains only pressurant gas supplied from external source.
  4. External tank heating is assumed to heat and evaporate liquid propellant only. Evaporation rate of propellant is calculated from heat transfer equation using tank wall and liquid propellant temperatures, heat transfer areas, latent heat of vaporization, and empirically determined coefficients.
  5. To simulate effects of transient and non-uniform temperatures through thick tank walls, the wall is modeled as having uniform temperature through 70% of the actual wall thickness where heat is transferred from the ullage gas; 30% of the wall thickness is modeled as thermally isolated from remaining wall.
  6. 740 BTU/hr-ft<sup>2</sup>-R for GH over LH and 520 BTU/hr-ft<sup>2</sup>-R for GN over LOX added to calculated convective heat transfer coefficient from Ref. 34 correlations to simulate effects of mixing between ullage gas and cryogenic propellant; these resulted in approximate 10% increase in required pressurant gas.
  7. Ullage gas modeled as having linear vertical temperature profile with temperature at top of region equal to entering pressurant gas temperature and temperature at bottom of region equal to saturation temperature of propellant; Mean ullage gas temperature used to calculate heat transfer at ullage gas boundaries with tank wall is average of temperatures at top and bottom of ullage gas region.
  8. During rapid change in tank pressure, mass transfer across ullage-gas-to-cryogenic-propellant interface is product of ullage volume and ullage gas density change based on net difference between new tank pressure and propellant saturation pressure.
  9. Natural convection correlation used with time of pressurant gas entry, thermal properties of ullage gas and tank wall, tank wall thickness and inside diameter to compute ratio of actual to maximum total heat in tank wall; Maximum total heat in tank wall is when all of tank wall is at temperature of the incoming pressurant gas; Coefficients and exponents in the correlation to compute ratio of actual to maximum total heat in tank wall are derived from curvefits of empirical data.

Three studies<sup>14,88,91</sup> employ a more complex method for modeling the temperature of the tank wall section in contact with ullage gas. For the models presented in these studies, the tank wall is modeled as finite discrete segments vertically stacked from the top to the bottom of the tank. Those tank segments in contact with liquid propellant are set at temperatures equal to that of the liquid propellant. The tank segments in contact with the ullage gas are each modeled as nodes with each having uniform temperature and thermal properties.

All models presented by reference citations in Table 6 were used for subcritical tank pressure conditions with the exception of References 79 and 80.

## **F. Multiple Discrete Fluid Segment Models**

In contrast, and as an intended enhancement to the LMFR computer models, other models have been developed and used where one or more intra-tank fluid regions are subdivided into discrete horizontal segments in order to provide a more accurate representation of temperature gradients in the intra-tank fluid regions. Each segment is treated as a small bulk mass of fluid having uniform properties throughout.

Table 7 presents a listing of studies where subdivision of the ullage gas region, cryogenic (liquid) propellant region, or both regions into discrete finite segments was employed in computer programs used to predict pressurant gas requirements or pressure rise rates in cryogenic propellant tanks for pressurization or pressurized propellant expulsion processes. With the exception of Ref. 93, all of the Multiple Discrete Fluid Segment (MDFS) Models cited in Table 7 subdivide the ullage gas region into vertically stacked discrete finite horizontal segments. Each segment is modeled as having uniform properties where a portion of the pressurant gas entering the ullage uniformly mixes with gas already in this segment. This was done in order to provide a more accurate representation of the vertical temperature gradients known from empirical data to exist in the cryogenic tank ullage gas regions and adjacent tank walls, as illustrated in references cited in Tables 3 and 4.

Although the MDFS models involve a higher level of computer program complexity, significantly increased numbers of repetitive and iterative calculations, increased computing time, and increases in computer memory requirements, the developers of these models deemed that this was necessary to provide consistently accurate model results for a wide variety of cryogenic tank sizes and geometries as well as for a wide variety of operating conditions.

The majority of MDFS computer models in Table 7 treat the cryogenic (liquid) propellant region as a single lumped mass having uniform properties throughout the region. Most of these models also apply the assumption of negligible heat transfer between propellant region and adjacent tank walls due to a negligible temperature difference between propellant region and tank walls adjacent to this region.

With regards to the modeling of transient heat conduction in the tank walls, all models presented by the cited references on Table 7 apply the assumption of near zero temperature gradient through the thickness of the tank wall.

For all of the models referenced in Table 7, except Ref. 93, the tank wall is subdivided into vertically-stacked finite segments. For all of these models, the heat transfer between any two adjacent wall segments is assumed to be negligible.

Results obtained with the MDFS computer program models referenced in Table 7 provide good to excellent predictions of pressurant gas requirements and associated collapse factors when compared to corresponding empirical data. For all models, predicted pressurant gas flow rates or collapse factors are generally within 14% of corresponding empirical data.

When initially comparing Tables 6 and 7, the MDFS models (cited in Table 7) appear to provide little or no improvements over the LMFR models (cited in table 6). However, the former models are evaluated for accuracy for a much wider range of tank geometries and sizes ranging from 17.7-gallons to thousands and tens of thousands of gallons while the latter models were only evaluated for vertical cylinder tanks of 500- gallon and smaller

**Table 7 Summary Data for Multiple Discrete Fluid Segment (MDFS) Models**

Reference Citation	Heat Transfer						Mass Transfer		Model Errors Compared to Empirical Data
	Ullage Gas to Wall	Propellant to Wall	Ullage Gas to Propellant	Intra-Ullage-Gas Segment-to-Segment	Intra-Propellant Segment-to-Segment	External Tank Wall	Ullage Gas to Propellant	Intra-Ullage-Gas Segment-to-Segment	
3	NLC, NC & FC	NLC, NC	NLC, NC, FC	EC & EFC	EC	Adiabatic Outer Wall Modeled	N/A, Assumed to be Zero	No Mass Transfer other than Pressurant Gas Entry	-13.0 to +1.0% for Test 004A +2.9 to +14.0% for Test 0027A -2.7 to +9.1% for Test 0029B
17 and 18	NLC, NC	N/A, No Heat Transfer Assumed	NLC, NC (Same correlation as Ref. 91)	EC	N/A, Uniform Propellant Region Modeled	Adiabatic Outer Wall Modeled	(1)	No Mass Transfer other than Pressurant Gas Entry	Range: -2.73 to 19.48%; Mean: 5.29%; Std. Dev.: 5.56%; 19 Tests Compared
23	NLC, NC	NLC, NC	EC	EC	EC	NLC, NC, Note 2	(1)	(6)	<5%
30	NLC, NC	N/A, No Heat Transfer Assumed	NLC, NC	N/A, No Heat Transfer Assumed	N/A, Uniform Propellant Region Modeled	Input Heat Flux	N/A, Assumed to be Zero	No Mass Transfer other than Pressurant Gas Entry	Range: -8.23 to 12.04%; Mean: 2.22%; Std. Dev.: 6.05%; 10 Tests Compared
34	NLC, NC & FC	NLC, NC	NLC, NC & FC	EC	EC	NLC, NC & Radiation, Note 1	(6)	(6)	Range: Approx. -30 to 12%; Mean: 0.1 to 2.3%; Std. Dev.: 10.9 to 8.5%; 11 Tests Compared
93	No Heat Transfer Assumed	EC	EC (liquid side only)	N/A	EC	Input Heat Flux	(1)	N/A; Ullage Gas at Uniform Temp.	No Comparisons Presented
94	NLC, NC & FC	NLC, NC	NLC, NC & FC	EC	EC	NLC, NC & Radiation, Note 1	(1) and (6)	(6)	Comparisons not presented; ~10% Max. Cumulative Error; ~20% Max. Instantaneous Error from Nein and Thompson (1966)
95	NLC, NC & FC	NLC, NC	NLC, NC & FC	EC	EC	Unknown	(1)	Unknown	~10% for Test 130-9; ~10 to 12% for Test 130-6; ~5% for Test 6E
96	NLC, NC & FC	No Heat Transfer Assumed	NLC, NC (Same correlation as Ref. 91)	EC	N/A, Uniform Propellant Region Modeled	Input Heat Flux	Not Discussed	No Mass Transfer other than Pressurant Gas Entry	0.5 to 16.0% Error for Tank Pressurization; 7.0 to 12.4% Error for Propellant Expulsion

**Key:**

- NLC = Newton's Law of Cooling
- NC = Natural (Free) Convection; Ref. 34 correlations unless noted otherwise
- FC = Forced Convection; correlation presented in "Combined Natural and Forced Convection Correlations" section
- EC = Equivalent Conduction; thermal conductivity and slope of temperature gradient across finite segment/element at boundary
- EFC = Equivalent Forced Convection (and Mixing); similar to correlation presented in "Combined Natural and Forced Convection Correlations" section
- (1) = First Mass Transfer Computation Technique, from "Mass Transfer Correlations" Section of Chapter II in Ref. 3
- (6) = Sixth Mass Transfer Computation Technique, from "Mass Transfer Correlations" Section of Chapter II in Ref. 3

**Notes:**

1. Equivalent conductance based on natural convection and radiation heat transfer is used; this parameter is calculated from equation using empirically derived constants, bottle wall temperature and ambient air temperature, and these temperatures raised to the fourth power
2. Equivalent conductance based on natural convection only; correlation not presented

capacities, except for the one 2400-gallon spherical LH tank expulsion test in one study<sup>79</sup>. Also, each of the studies cited in Table 6 where error ranges are more favorable, employed correlations with coefficients and exponents determined to provide best results for a single tank configuration and a limited range of test conditions. Therefore, the MDFS collapse factor analysis computer programs generally provide a much better assurance that “good” to “excellent” collapse factor predictions will result.

## G. Internal Tank Heat Transfer Correlations

Many of the models described herein involve the computation and use of heat transfer rates across fluid regional boundaries. The majority of these models utilize correlations that determine heat transfer rates at the ullage-gas-to-tank-wall boundaries while considering heat transfer at the interface between ullage gas and cryogenic (liquid) propellant to be negligibly small. A smaller select group of models employ correlations for heat transfer across this interface. An even smaller select group of models evaluate and account for heat transfer rates across boundaries between cryogenic propellant and tank walls, but the vast majority of models are either based on the assumption of negligible heat transfer at cryogenic-propellant-to-tank-wall boundaries where temperatures of propellant and adjacent tank walls or wall segments are considered to be virtually equal.

### 1. Natural Convection Correlations

For the majority of LMFR and MDFS computer models, natural or free convection heat transfer is treated as being the only mode of heat transfer at ullage gas and cryogenic propellant region boundaries.

A general natural convection correlation is utilized in virtually all of the models cited in Sections IV.C. through IV.F. It is based on Nusselt number equated as the product of an empirically derived constant and the Rayleigh number raised to an exponential power. The constants and exponential powers are those used for heated or cooled horizontal, vertical, and inclined vertical flat plate correlations as well as correlations used for domed enclosures in some cases. A number of the references cited on Tables 3, 4, 5, 6, and 7 as well as in Sections IV.C. through IV.F. state the values used for constants and exponential powers.

In addition to the general natural convection Nusselt number correlation described above, a number of other Nusselt number correlations of different forms have been developed and presented in prior literature<sup>17,18,44,79,97-102</sup>. All of the presented Nusselt number correlations generally use fluid properties and characteristic dimensions.

### 2. Combined Natural and Forced Convection Correlations

The majority of numerical finite difference computer models presented by studies cited in Tables 6 and 7 are based on all natural convection heat transfer at all or selected fluid regional boundaries. The reference citations in Table 7 that indicate natural and forced convection (“NC” and “FC”) for ullage-gas-to-wall heat transfer combine the effects of natural and forced convection at boundaries of the discrete horizontal segments in the ullage gas region as indicated by this table. For these models, the total equivalent convective heat transfer coefficients (or Nusselt numbers) at ullage-gas-to-tank-wall and at ullage-gas-to-cryogenic-propellant boundaries are equated as the sum of forced and natural convection components.

In contrast, two studies<sup>92,103</sup> recommend using the higher of the natural and forced convective heat transfer coefficients to determine rate of heat transfer at ullage-gas-to-wall and ullage-gas-to-propellant boundaries. For combined forced and natural convection heat transfer processes, Ref. 87 recommends the following Nusselt number correlation

$$Nu_T = \left[ Nu_L^n + Nu_F^n \right]^{1/n} \quad (1)$$

For the above correlation, the subscripts “F,” “L,” and “T” represent forced, natural (free), and total equivalent combined (forced and natural) convection respectively. In Ref. 87, the exponent “n” is generally taken to have a value of three (for non-transverse flows) while selected studies in Table 7, where “NC & FC” are column entries, essentially set “n” to unity. For cases where the forced convection effects oppose the natural convection effects

(forced convection alone would cause fluid to flow in direction opposite to flow direction if natural convection was acting alone), the plus sign in Equation (1) would change to a minus sign.

In the references in Table 7 where forced convection heat transfer effects are modeled for heat transfer between ullage gas and tank walls, the forced convective heat transfer coefficient is based on a Nusselt number correlation. This correlation equates Nusselt number to the product of a constant, Reynolds and Prandtl numbers of entering pressurant gas raised to exponential powers of 0.8 and 0.33 respectively, and an exponential decay factor. The exponential decay factor is based on the horizontal and vertical distances between location(s) on tank wall under evaluation and closest point where pressurant gas enters the tank ullage. As either or both of these distances increase, this factor decreases in value.

For references in Table 7 where effects of forced convection are modeled at the boundary between ullage gas and cryogenic (liquid) propellant, a similar correlation is used to calculate the forced convective heat transfer coefficient on the ullage gas side of this boundary.

## V. Conclusion

Empirical collapse factor data as well as methods and computer based models used to analytically determine/predict collapse factors in cryogenic propellant tanks have been presented. Additionally, other phenomena, including temperature distributions and inter-region mass transfer which affect collapse factors, have been described. Results show that collapse factors vary widely depending on tank size and configuration, propellant and pressurant gas species, and operating conditions. Methods and models used to analytically determine collapse factors also show varied levels of accuracy when compared with empirically determined collapse factors. The LMFR and MDFS models show the best results with the latter model providing best accuracy over a wide variety of conditions as it accounts for most or all phenomena known to significantly affect collapse factors.

Nearly all collapse factor studies to date cover cases where cryogenic tank operating pressures are well below the critical pressure of the cryogenic propellant, so this propellant is in the liquid phase and a distinct liquid-to-gas boundary exists between propellant and ullage gas. A few selected cases cover operating pressures that are near or above this critical pressure where a distinct boundary between propellant and ullage gas may not exist. Collapse factor data for these cases are limited.

## Acknowledgements

The authors would like to acknowledge many of the authors who produced the works listed in the references, Mississippi State University, NASA Stennis Space Center, key faculty and staff in these organizations, and family members and friends who have provided key support in making this article possible.

## References

<sup>1</sup>Sutton, G. P., *Rocket Propulsion Elements; An Introduction to the Engineering of Rockets, 6<sup>th</sup> Edition*, John Wiley & Sons, New York, NY, 1992.

<sup>2</sup>Barber, H. E., "Advanced Pressurization Systems Technology Program Final Report," Technical Report AFRPL-TR-66-278, Edwards, CA, 1966.

<sup>3</sup>de Quay, L., "*Validated Prediction of Pressurant Gas Requirements in Cryogenic Run Tanks at Subcritical and Supercritical Pressures*," UMI Dissertation Publishing, Number 3386300, ProQuest LLC, Ann Arbor, MI, 2009.

<sup>4</sup>DeWitt, R. L., & McIntire, T. O., "Pressurant Requirements for Discharge of Liquid Methane from a 1.52-Meter- (5-ft-) Diameter Spherical Tank Under Both Static and Slosh Conditions," NASA-TN-D-7638, 1974.



<sup>5</sup>Epstein, M., & Anderson, R. E., "An Equation for the Prediction of Cryogenic Pressurant Requirements for Axisymmetric Propellant Tanks," *Advances in Cryogenic Engineering*, Vol. 13, ed. Timmerhaus, K. D., Plenum Press, New York, NY, 1968, pp. 207-214.

<sup>6</sup>Lacovic, R. F., "Comparison of Experimental and Calculated Helium Requirements for Pressurization of a Centaur Liquid Oxygen Tank," NASA-TM-X-2013, 1970.

<sup>7</sup>Nein, M. E., & Head, R. R., "Experiences with Pressurized Discharge of Liquid Oxygen from Large Flight Vehicle Propellant Tanks," *Advances in Cryogenic Engineering*, Vol. 7, ed. Timmerhaus, K. D., Plenum Press, New York, NY, 1962, pp. 244-250.

<sup>8</sup>Shelburne, L., "E-8 Turbopump Testing" Facsimile Transmission dated June 4, 1990, Pratt and Whitney Advanced Launch System Space Transportation Engine Program Coordination Memo No. NSO-020-14, 1990.

<sup>9</sup>Cowart, E. G., "Saturn V S-II Final Propulsion System Performance Prediction Flight SA-503, Vol. II of III," Boeing Space Division Document No. D5-15530-3A, July 1968.

<sup>10</sup>"Main Propellant Tank Pressurization System Study and Test Program, Vol. I, Liquid Hydrogen and Liquid Oxygen," Lockheed Report ER-5238, 1961.

<sup>11</sup>Bourgarel, M., Clement, R., Segel, M., "A Cryogenic Propellant Tank Pressurization Analysis," *Proceedings of the 2<sup>nd</sup> International Cryogenic Engineering Conference*, Iliffe Science and Technology Publications, Guildford, UK, 1968, pp. 89-101.

<sup>12</sup>Coxe, E. F., & Tatom, J.W., "Analysis of the Pressurizing Gas Requirements for an Evaporated Propellant Pressurization System," *Advances in Cryogenic Engineering*, Vol. 7, ed. Timmerhaus, K. D., Plenum Press, New York, NY, 1962, pp. 234-243.

<sup>13</sup>Hardy, T. L., & Whalen, M. V., "Slush Hydrogen Propellant Production, Transfer, and Expulsion Studies at the NASA K-Site Facility," AIAA Paper 1991-3550, Also NASA-TM-105191, 1991.

<sup>14</sup>Mandell, D. A., & Roudebush, W. H., "Parametric Investigation of Liquid Hydrogen Tank Pressurization During Outflow," NASA-TN-D-2797, 1965.

<sup>15</sup>Moore, R. W., Fowle, A. A., Bailey, B. M., Ruccia, F. E., & Reid, R. C., "Gas Pressurized Transfer of Liquid Hydrogen," *Advances in Cryogenic Engineering*, Vol. 5, ed. Timmerhaus, K. D., Plenum Press, New York, NY, 1960, pp. 450-459.

<sup>16</sup>Stochl, R. J., & DeWitt, R. L., "Pressurant Gas Requirements for the Pressurized Discharge of Liquid Hydrogen from Propellant Tanks," AIAA Paper 1969-526, 1969.

<sup>17</sup>Stochl, R. J., Maloy, J. E., Masters, P. A., & DeWitt, R. L., "Gaseous-Helium Requirements for the Discharge of Liquid Hydrogen from a 1.52-Meter- (5-Ft-) Diameter Spherical Tank," NASA-TN-D-5621, 1970.

<sup>18</sup>Stochl, R. J., Maloy, J. E., Masters, P. A., & DeWitt, R. L., "Gaseous-Helium Requirements for the Discharge of Liquid Hydrogen from a 3.96-Meter- (13-Ft-) Diameter Spherical Tank," NASA-TN-D-7019, 1970.

<sup>19</sup>Stochl, R. J., Van Dresar, N. T., & Lacovic, R. F., "Autogenous Pressurization of Cryogenic Vessels Using Submerged Vapor Injection," *Advances in Cryogenic Engineering*, Vol. 37, Part B, ed. Fast, R. W., Plenum Press, New York, NY, pp. 1273-1280; Also NASA-TM-104516, 1991.

<sup>20</sup>Van Dresar, N. T. & Stochl, R. J., "Pressurization and Expulsion of a Flightweight Liquid Hydrogen Tank," AIAA Paper 1993-1966, Also NASA-TM-106427, 1993.

<sup>21</sup>Whalen, M. V., & Hardy, T. L., "Slush Hydrogen Pressurized Expulsion Studies at the NASA K-Site Facility," AIAA Paper 1992-3385, Also NASA-TM-105597, 1992.

<sup>22</sup>Arnett, R. W. & Voth, R. O., "A Computer Program for the Calculation of Thermal Stratification and Self-Pressurization in a Liquid Hydrogen Tank," NASA-CR-2026, 1972.

<sup>23</sup>Baral, H. S., "Liquid Propellant Pressurization System," *Journal of the Institution of Engineers, Mechanical Engineering Division*, Calcutta, India, Vol. 68, No. 5, 1988, pp. 127-131.

<sup>24</sup>Bowersock, D. C., & Reid, R. C., "An Analytical Method for Estimating Gas Requirements in the Pressurization and Transfer of Cryogenic Fluids," *Advances in Cryogenic Engineering*, Vol. 6, ed. Timmerhaus, K. D., Plenum Press, New York, NY, 1961, pp. 261-271.

<sup>25</sup>Cady, E. C., Flaska, T. L., & Worrell, P. K., "In-Tank Thermodynamics of Slush Hydrogen for the National Aerospace Plane," *Advances in Cryogenic Engineering*, Vol. 35, Part B, ed. Fast, R. W., Plenum Press, New York, NY, 1990, pp. 1755-1766.

<sup>26</sup>Clark, J. A., "A Review of Pressurization, Stratification, and Interfacial Phenomena," *International Advances in Cryogenic Engineering*, Vol. 11, ed. Timmerhaus, K.D., Plenum Press, New York, NY, 1965, pp. 259-283.

<sup>27</sup>Hasan, M. M. & Lin, C. S., "A Numerical Study of the Direct Contact Condensation on a Horizontal Surface," AIAA Paper 1991-1307, Also NASA-TM-102437, 1991.

<sup>28</sup>Kendle, D. W., "Ullage Mixing Effects on Tank Pressurization Performance," AIAA Paper 1970-681, 1970.

- <sup>29</sup>Nein, M. E., & Thompson, J. F., "Experimental and Analytical Studies of Cryogenic Propellant Tank Pressurization," *Proceedings of the Conference on Propellant Tank Pressurization and Stratification*, Vol. 2, NASA Marshall Space Flight Center, Huntsville, AL, 1965, pp. 29-54.
- <sup>30</sup>Roudebush, W. H., "An Analysis of the Problem of Tank Pressurization During Outflow," NASA-TN-D-2585, 1965.
- <sup>31</sup>Swalley, F. E., Ward, W. D., & Toole, L. E., "Low Gravity Fluid Behavior and Heat Transfer Results from the S-IVB-203 Flight," *Proceedings of the Conference on Long Term Cryo-Propellant Storage in Space*, Oct. 12-13, 1966, NASA Marshall Space Flight Center, Huntsville, AL, 1966, pp. 213-232.
- <sup>32</sup>Beduz, C., Rebiai, R., & Scurlock, R. G., "Thermal Overfill, And The Surface Vaporisation of Cryogenic Liquids Under Storage Conditions," *Advances in Cryogenic Engineering*, Vol. 29, ed. Fast, R. W., 1984, pp. 793-803.
- <sup>33</sup>Gluck, D. F., & Kline, J. F., "Gas Requirements in Pressurized Transfer of Liquid Hydrogen," *Advances in Cryogenic Engineering*, Vol. 7, ed. Timmerhaus, K. D., Plenum Press, New York, NY, 1962, pp. 219-233.
- <sup>34</sup>Nein, M. E., & Thompson, J. F., "Experimental and Analytical Studies of Cryogenic Propellant Tank Pressurant Requirements," NASA-TN-D-3177, 1966.
- <sup>35</sup>Lemmon, E. W., Huber, M. L., & Mc Linden, M. O., "Reference Fluid Thermodynamic and Transport Properties (REFPROP)," NIST Standard Reference Database 23, Version 8.0, April 2007.
- <sup>36</sup>Al-Najem, N. M., Al-Marafie, A. M., & Ezuddin, K. Y., "Analytical and Experimental Investigation of Thermal Stratification in Storage Tanks," *International Journal of Energy Research*, Vol. 17, 1993, pp. 77-88.
- <sup>37</sup>Barnett, D. O., "Liquid Nitrogen Stratification Analysis and Experiments in a Partially Filled, Spherical Container," *Advances in Cryogenic Engineering*, Vol. 13, ed. Timmerhaus, K. D., Plenum Press, New York, NY, 1967, pp. 174-187.
- <sup>38</sup>Barnett, D. O., Winstead, J. W., & McReynolds, L. S., "An Investigation of Liquid-Hydrogen Stratification in a Large Cylindrical Tank of the Saturn Configuration," *Advances in Cryogenic Engineering*, Vol. 11, ed. Timmerhaus, K. D., Plenum Press, New York, NY, 1964, pp. 314-324.
- <sup>39</sup>Fan, B. C., Chu, J. C., & Scott, L. E., "Thermal Stratification in Closed Cryogenic Containers," *Advances in Cryogenic Engineering*, Vol. 14, ed. Timmerhaus, K. D., Plenum Press, New York, NY, 1969, pp. 249-257.
- <sup>40</sup>Ghaddar, N. K., Al-Marafie, A. M., & Al-Kandari, A., "Numerical Simulation of Stratification Behavior in Thermal Storage Tanks," *Applied Energy*, Vol. 32, No. 3, Applied Science Publishers, Barking, UK, 1989, pp. 225-239.
- <sup>41</sup>Gursu, S., Sherif, S. A., Veziroglu, T. N., & Sheffield, J. W., "Analysis and Optimization of Thermal Stratification and Self-Pressurization Effects in Liquid Hydrogen Storage Systems – Part 1: Model Development and Part 2: Model Results and Conclusions," *Journal of Energy Resources Technology*, Vol. 115, No. 3, Sept. 1993, pp. 221-231.
- <sup>42</sup>Kharin, V. M., Ryazhskikh, V. I., Zavadskikh, R. M., "Stratification of a Cryogenic Liquid in a Reservoir in the Case of Circulation Cooling," *Journal of Engineering Physics*, Vol. 60, No. 3, March 1991, Plenum Publishing Corporation, 1991, pp. 336-338.
- <sup>43</sup>Liebenburg, D. H., & Edeskuty, F. J., "Pressurization Analysis of a Large-Scale Liquid Hydrogen Dewar," *International Advances in Cryogenic Engineering*, Vol. 11, ed. Timmerhaus, K. D., Plenum Press, New York, NY, 1965, pp. 284-289.
- <sup>44</sup>Neff, B. D., & Chiang, C. W., "Free Convection in a Container of Cryogenic Fluid," *Advances in Cryogenic Engineering*, Vol. 12, ed. Timmerhaus, K. D., Plenum Press, New York, NY, 1967, pp. 112-124.
- <sup>45</sup>Olsen, W. A., "Experimental and Analytical Investigation of Interfacial Heat and Mass Transfer in a Pressurized Tank Containing Liquid Hydrogen," NASA-TN-D-3219, 1966.
- <sup>46</sup>Ordin, P. M., Weiss, S., & Christenson, H., "Pressure-Temperature Histories of Liquid Hydrogen Under Pressurization and Venting Conditions," *Advances in Cryogenic Engineering*, Vol. 5, ed. Timmerhaus, K. D., Plenum Press, New York, NY, 1960, pp. 481-486.
- <sup>47</sup>Schmidt, A. F., Purcell, J. R., Wilson, W. A., & Smith, R. V., "An Experimental Study Concerning the Pressurization and Stratification of Liquid Hydrogen," *Advances in Cryogenic Engineering*, Vol. 5, ed. Timmerhaus, K. D., Plenum Press, New York, NY, 1960, pp. 487-497.
- <sup>48</sup>Segel, M. F., "Experimental Study of the Phenomena of Stratification and Pressurization of Liquid Hydrogen," *International Advances in Cryogenic Engineering*, Vol. 11, ed. Timmerhaus, K. D., Plenum Press, New York, NY, 1965, pp. 308-313.

<sup>49</sup>Tanyun, Z., Zhongping, H., & Shimo Li (1996). "Numerical Simulation of Thermal Stratification in Liquid Hydrogen," *Advances in Cryogenic Engineering*, Vol. 41, Part A, ed. Kittel, P., Plenum Press, New York, NY, pp. 155-161.

<sup>50</sup>Atkinson, M. C. M., Beduz, C., Rebiai, R., & Scurlock, R. G., "Heat and Evaporative Mass Transfer Correlation at the Liquid-Vapour Interface of Cryogenic Liquids," *Proceedings of the 10<sup>th</sup> Cryogenic Engineering Conference*, ed. Collan, et al., Butterworth Publishing Co., Northamptonshire, UK, 1984, pp. 95-97.

<sup>51</sup>Clark, J. A., Van Wylen, G. J., & Fenster, S. K., "Transient Phenomena Associated with the Pressurized Discharge of a Cryogenic Liquid from a Closed Vessel," *Advances in Cryogenic Engineering*, Vol. 5, ed. Timmerhaus, K. D., Plenum Press, New York, NY, 1960, pp. 467-480.

<sup>52</sup>Tuttle, J., DiPirro, M. J., & Shirron, "Thermal stratification of liquid helium in the SHOOT Dewars," *Cryogenics*, Vol. 34, No. 5, Butterworth-Heinemann, Oxford, UK, 1994, pp. 369-374.

<sup>53</sup>Zenner, G. H., "The Storage and Handling of Cryogenic Liquids," *Progress in Cryogenics*, Vol. 2, ed. Mendelssohn, K., Academic Press, Inc., New York, NY, 1960.

<sup>54</sup>"Main Propellant Tank Pressurization System Study and Test Program, Vol. III, Design Handbook," Lockheed Report ER-5296, Vol. III, 1961.

<sup>55</sup>Bowersock, D. C., Gardner, R. W., & Reid, R. C., "Pressurized Transfer of Cryogenic Liquids," *Advances in Cryogenic Engineering*, Vol. 4, ed. Timmerhaus, K. D., Plenum Press, New York, NY, 1960, pp. 342-356.

<sup>56</sup>Greenfield, S., "Dilution of Cryogenic Liquid Rocket Propellants During Pressurized Transfer," *Proceedings of the 1957 Cryogenic Engineering Conference*, ed. Timmerhaus, K. D., National Bureau of Standards, Boulder, CO, 1958, pp. 136-148.

<sup>57</sup>Epstein, M., "Prediction of Liquid Hydrogen and Oxygen Pressurant Requirements," *International Advances in Cryogenic Engineering*, Vol. 11, ed. Timmerhaus, K. D., Plenum Press, New York, NY, 1965, pp. 303-307.

<sup>58</sup>Bailey, W. J., Weiner, S. P., Beckman, D. H., Dennis, M. F., & Martin, T. A., "Cryogenic On-Orbit Liquid Depot Storage, Acquisition and Transfer Satellite (COLD-SAT)," NASA-CR-185247, 1990.

<sup>59</sup>Bailey, W. J. & Arif, H., "Cryogenic Fluid Management Investigations Using the CONE Flight Experiment," *Cryogenics*, Vol. 32, No. 2, 1992, pp. 220-229.

<sup>60</sup>Blatt, M. H., "Empirical Correlations for Pressure Rise in Closed Cryogenic Containers," *Journal of Spacecraft and Rockets*, Vol. 5, No. 6, 1968, pp. 733-735.

<sup>61</sup>Denisov, K. P., Lukovskij, A. P., Ledneva, L. P., Chuherov, A. I., Federov, V. I., "Experimental Study of the Effect of Gas Injection Velocity on Heat and Mass Transfer in the Gas Volume of a Tank," *Aviatsionnaia Tekhnika*, No. 1, 1981, pp. 84-86.

<sup>62</sup>Humphrey, J. C., "Pressurized Transfer of Cryogenic Fluids from Tanks in Liquid Nitrogen Baths," *Advances in Cryogenic Engineering*, Vol. 6, ed. Timmerhaus, K. D., Plenum Press, New York, NY, 1961, pp. 281-292.

<sup>63</sup>Kamat, D. V., & Abraham, W. H., "Pressure Collapse in Oxygen Storage under Zero-g," *Journal of Spacecraft and Rockets*, Vol. 5, No. 2, February 1968, pp. 184-188.

<sup>64</sup>Rotenburg, Y., "Numerical Simulation of Self Pressurization in a Small Cryogenic Tank," *Advances in Cryogenic Engineering*, Vol. 31, ed. Fast, R. W., Plenum Press, New York, NY, 1986, pp. 963-971.

<sup>65</sup>Van Dresar, N. T., Lin, C. S., & Hasan, M. M., "Self-Pressurization of a Flightweight Liquid Hydrogen Tank: Effects of Fill Level at Low Wall Heat Flux," AIAA Paper 1992-0818, Also NASA-TM-105411, 1992.

<sup>66</sup>Van Dresar, N. T., & Habermusch, M. S., "Thermodynamic Models for Bounding Pressurant Mass Requirements of Cryogenic Tanks," *Advances in Cryogenic Engineering*, Vol. 39, Part B, ed. Kittel, P., Plenum Press, New York, NY, 1994, pp. 1907-1914.

<sup>67</sup>Smith, I. E., "Cryogenic Rocket Propellants," *Progress in Cryogenics*, Vol. 3, ed. Mendelssohn, K., Academic Press, New York, NY, 1961.

<sup>68</sup>Aydelott, J. C., "Modeling of Space Vehicle Propellant Mixing," NASA-TP-2107, 1983.

<sup>69</sup>Bentz, M. D., Meserole, J. S., & Knoll, R. H., "Tank Pressure Control Experiment - A Low-G Mixing Investigation," AIAA Paper 1990-2376, 1990.

<sup>70</sup>Bentz, M. D., Meserole, J. S., & Knoll, R. H., "Jet Mixing in Low Gravity - Results of the Tank Pressure Control Experiment," AIAA Paper 1992-3060, 1992.

<sup>71</sup>Bentz, M. D. (1993). "Tank Pressure Control in Low Gravity by Jet Mixing," NASA-CR-191012.

<sup>72</sup>Chato, D.J., "Ground Testing on the Nonvented Fill Method of Orbital Propellant Transfer: Results of Initial Test Series," AIAA Paper 1991-2326, 1991.

<sup>73</sup>Chato, D. J., "Ground Testing for the No-Vent Fill of Cryogenic Tanks: Results of Tests for a 71 Cubic Foot Tank," AIAA Paper 1993-1967, 1993.

- <sup>74</sup>Meserole, J. S., Jones, O. S., & Fortini, A., "Mixing-Induced Fluid Destratification and Ullage Condensation," *NASA Lewis Research Center Microgravity Fluid Management Symposium Proceedings*, April 1, 1987, pp. 101-117.
- <sup>75</sup>Moran, M. E., Nyland, T. W., & Driscoll, S. L., "Hydrogen No-Vent Fill Testing in a 34 Liter (1.2 Cubic Foot) Tank," *Advances in Cryogenic Engineering*, Vol. 37, Part B, ed. Fast, R. W., Plenum Press, New York, NY, 1991, pp. 1257-1264.
- <sup>76</sup>Reaser, W. W., Wilson, E. L., & Smith, D. A., "Design of Cryogenic Fluid Systems in the S-IV Stage Propulsion System," *Annals of Reliability and Maintainability, Fourth Annual Reliability and Maintainability Conference*, 1965, pp. 367-374.
- <sup>77</sup>Schmidt, G. R., Carrigan, R. W., Hahs, J. E., Vaughan, D. A., & Foust, D. C., "No-Vent Fill Pressurization Tests Using a Cryogen Simulant," NASA-TM-103561, 1991.
- <sup>78</sup>Vaughan, D. A., Foust, D. C., & Schmidt, G. R., "Enhancement of the No-Vent Fill Process," AIAA Paper 1991-1842, 1991.
- <sup>79</sup>Hodge, B. K., & Koenig, K., "A PC-Based Collapse Factor Analysis for High Pressure Cryogenic Systems," dated July 1992, NASA Stennis Space Center Contract NAS13-330 Order No. 30., 1992 (shorter version with same title is also presented in AIAA Paper 1992-3683)
- <sup>80</sup>Ludwig, K. A., & Houghton, P. A. "Collapse Factor Analysis Final Report," Air Products and Chemicals, Inc. Report to NASA Stennis Space Center for CTF Project, June 20, 1989.
- <sup>81</sup>Vance, R. W., & Duke, W. M., *Applied Cryogenic Engineering*, John Wiley & Sons, New York, NY, 1962.
- <sup>82</sup>Van Dresar, N. T., "Prediction of Pressurant Mass Requirements for Axisymmetric Liquid Hydrogen Tanks," AIAA Paper 1995-2964, Also NASA-TM-106973, 1995.
- <sup>83</sup>Thompson, J. F., & Nein, M. E., "Prediction of Propellant Tank Pressurization Requirements by Dimensional Analysis," NASA-TM-X-53218, 1965.
- <sup>84</sup>Van Dresar, N. T. & Stochl, R. J., "Pressurization and Expulsion of Cryogenic Liquids: Generic Requirements for a Low-Gravity Experiment," NASA-TM-104417, 1991.
- <sup>85</sup>Wapato, P. G., Keeley, A. W., Jew, L. N., and Young, C. F., "Study of External Pressurization Systems for Cryogenic Storage Systems," NASA-CR-115205, 1971.
- <sup>86</sup>Riemer, D. H., & Scarlotti, R., "Supercritical Hydrogen Expulsion Utilizing an External Pressurization System," *Advances in Cryogenic Engineering*, Vol. 29, ed. Fast, R. W., Plenum Press, New York, NY, 1984, pp. 741-747.
- <sup>87</sup>Incropera, F. P., & DeWitt, D. P., *Introduction to Heat Transfer, 2<sup>nd</sup> Edition*, John Wiley & Sons, New York, NY, 1990.
- <sup>88</sup>"Main Propellant Tank Pressurization System Study and Test Program, Vol. IV, Computer Program," Lockheed Report ER-5296, Vol. IV, 1961.
- <sup>89</sup>Anderson, J. E., Scott, O. L., & Brady, H. F., "Advanced Pressurization Systems for Cryogenic Propellants," NASA-CR-54467, 1967.
- <sup>90</sup>Majumdar, A., & Steadman, T., "Numerical Modeling of Pressurization of a Propellant Tank," Draft Paper for the 37<sup>th</sup> AIAA Aerospace Sciences Meeting, 1998.
- <sup>91</sup>Momenthy, A. M., "Propellant Tank Pressurization-System Analysis," *Advances in Cryogenic Engineering*, Vol. 9, ed. Timmerhaus, K. D., Plenum Press, New York, NY, 1964, pp. 273-283.
- <sup>92</sup>Ring, E., *Rocket Propellant and Pressurization Systems*, Prentice-Hall, Englewood Cliffs, NJ, 1964.
- <sup>93</sup>Lin, C. S., & Hasan, M. M., "Self-Pressurization of a Spherical Liquid Hydrogen Storage Tank in a Microgravity Environment," AIAA Paper 1992-0363, Also NASA-TM-105372, 1992.
- <sup>94</sup>"FORTRAN Program for the Analysis of a Single Propellant Tank Pressurization System," Rocketdyne Report R-3936-1. Also NASA-CR-53305, 1963.
- <sup>95</sup>Epstein, M., Georgius, H. K., & Anderson, R. E., "A Generalized Propellant Tank-Pressurization Analysis," *International Advances in Cryogenic Engineering*, Vol. 11, ed. Timmerhaus, K. D., Plenum Press, New York, NY, 1965, pp. 290-302.
- <sup>96</sup>Masters, P. A., "Computer Programs for Pressurization (Ramp) and Pressurized Expulsion from a Cryogenic Liquid Propellant Tank," NASA-TN-D-7504, 1974.
- <sup>97</sup>Chen, I. M. & Anderson, R. E., "A Thermal Stratification Model of a Cryogenic Tank at Supercritical Pressures," *Advances in Cryogenic Engineering*, Vol. 17, ed. Timmerhaus, K. D., Plenum Press, New York, NY, 1972, pp. 475-486.
- <sup>98</sup>Ede, A. J., "Advances in Free Convection," *Advances in Heat Transfer*, Vol. 4, eds. Irvine, T. F., & Hartnett, J. P., Academic Press, New York, NY, 1967, pp. 1-47.

<sup>99</sup>Gebhart, B., "Natural Convection Flows and Stability," *Advances in Heat Transfer*, Vol. 9, eds. Irvine, T. F., & Hartnett, J. P., Academic Press, New York, NY, 1973, pp. 273-297.

<sup>100</sup>Ostrach, S., "Natural Convection in Enclosures," *Advances in Heat Transfer*, Vol. 8, eds. Hartnett, J. P. & Irvine, T. F., Academic Press, Inc., New York, NY, 1972, pp. 161-227.

<sup>101</sup>Polyakov, A. F., "Heat Transfer under Supercritical Pressures," *Advances in Heat Transfer*, Vol. 21, eds. Hartnett, J. P., Irvine, T. F., Cho, Y. I., Academic Press, New York, NY, 1991.

<sup>102</sup>Raithby, G. D., & Hollands, K. G. T., "A General Method of Obtaining Approximate Solutions to Laminar and Turbulent Free Convection Problems," *Advances in Heat Transfer*, Vol. 11, eds. Irvine, T. F. & Hartnett, J. P., Academic Press, New York, NY, 1975, pp.265-315.

<sup>103</sup>Wulff, W., & Schipma, P., "Design Guide for Pressurized Gas Systems; Task 7," ITT Research Institute Report No, ITTRI-C6070-20, 1967.

# **A HISTORY OF COLLAPSE FACTOR MODELING AND EMPIRICAL DATA FOR CRYOGENIC PROPELLANT TANKS**

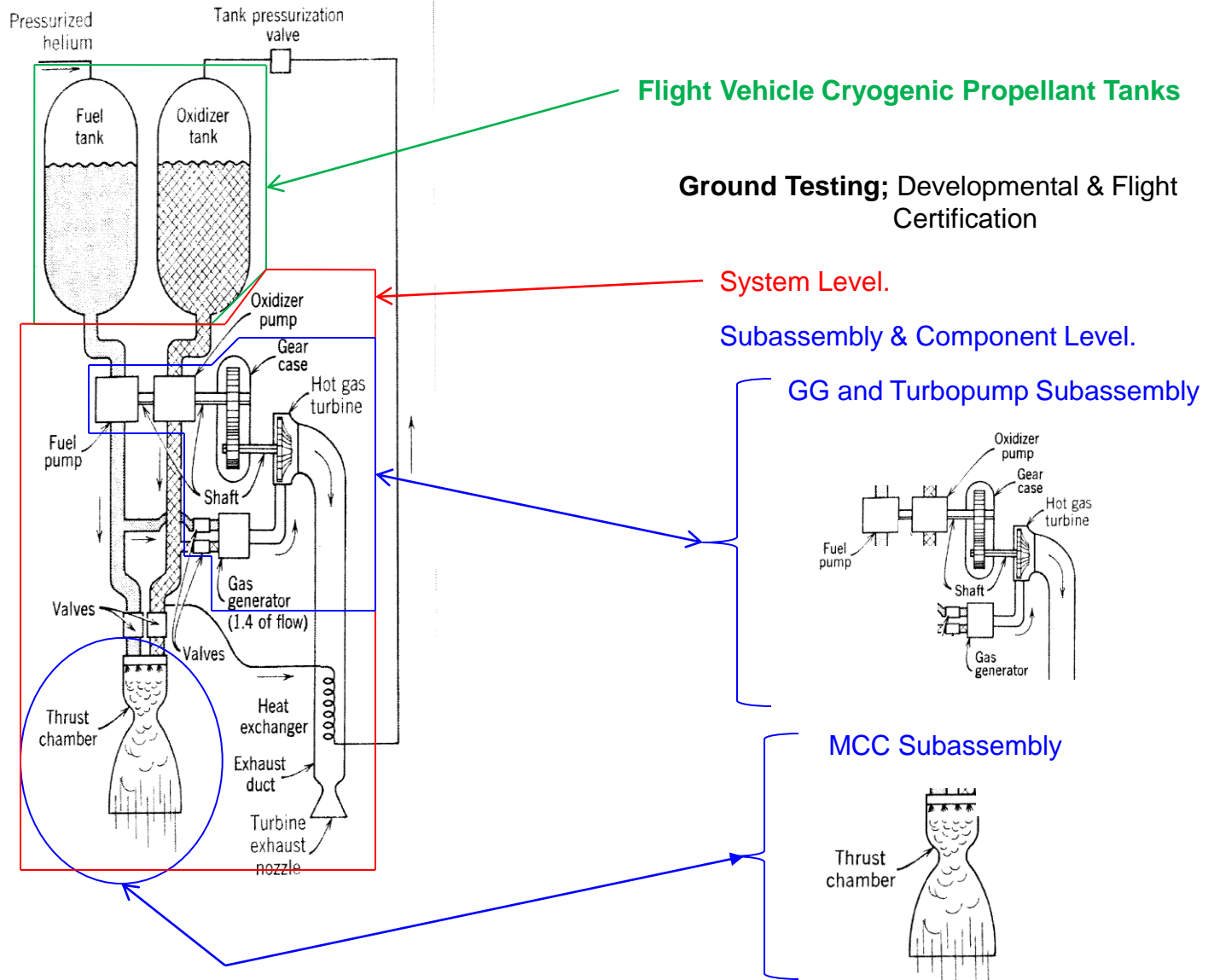
**Authors: Laurence de Quay, Ph.D., P.E., NASA Stennis Space Center  
B. Keith Hodge, Ph.D., P.E., Mississippi State University**

**The contents of this presentation are based on portions of a Ph.D. dissertation by the principal author, Laurence de Quay, while a student at Mississippi State University**

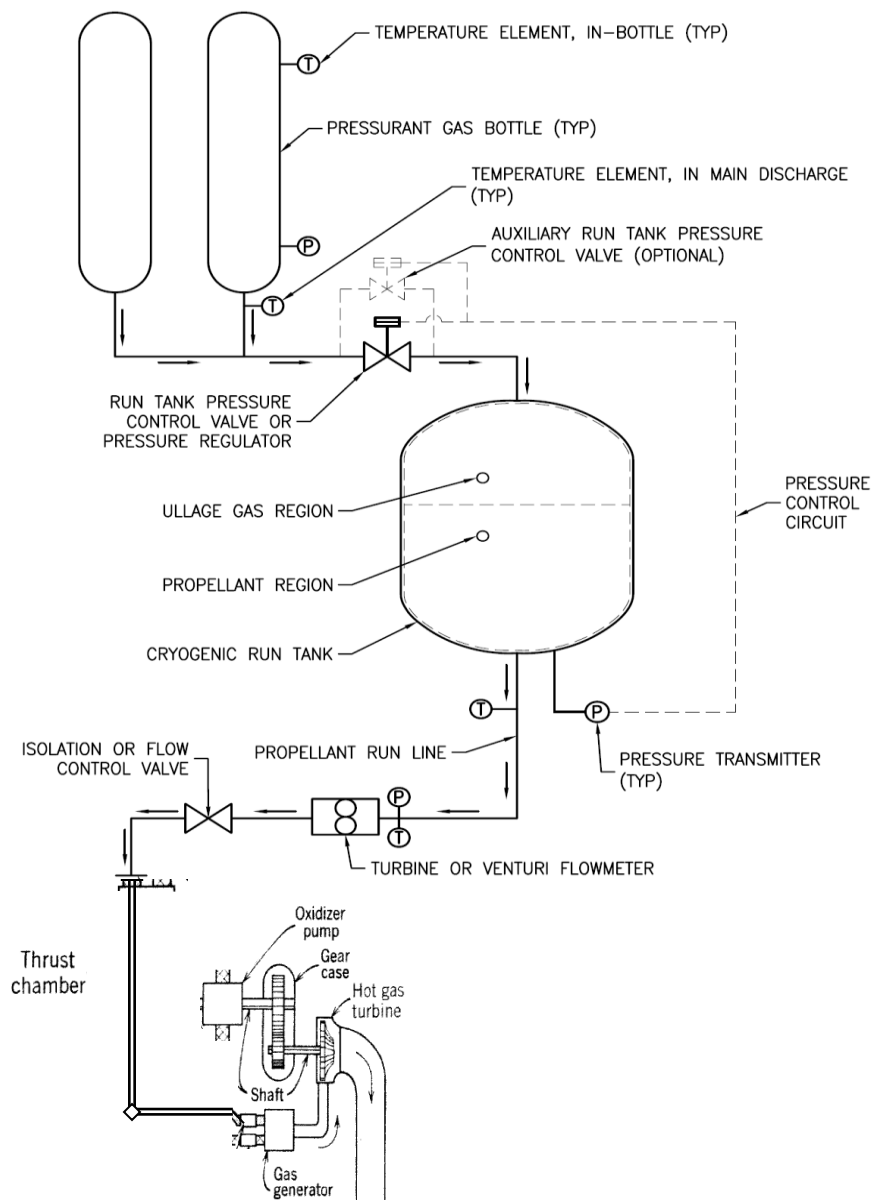
**The purpose of this paper is to present a summary and selected details of prior literature that document the ullage and pressurant gas collapse phenomenon, collapse factor, associated with cryogenic propellant tanks. Additionally, other literature that present studies and results of heat and mass transfer processes, related to or providing important insights or analytical methods for the studies of collapse factor, are presented.**



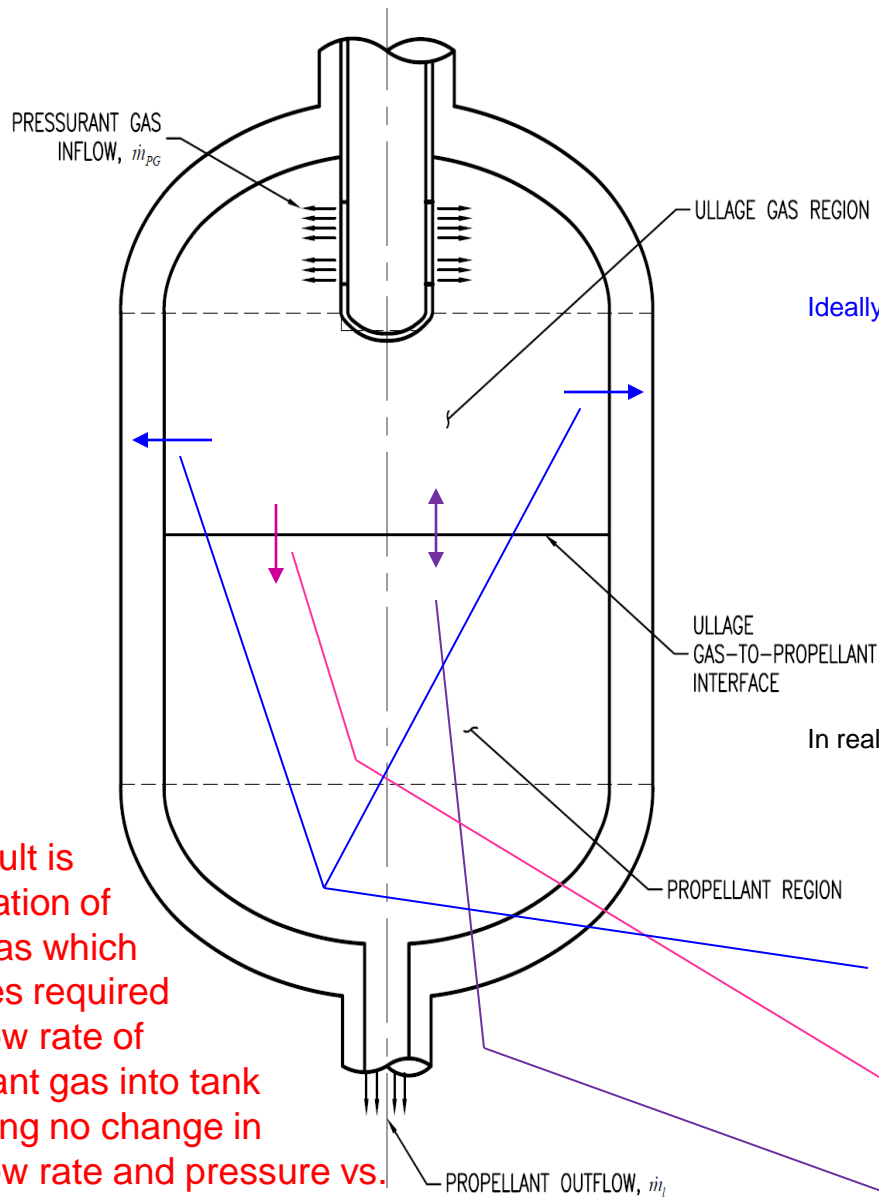
# Background: Liquid Propellant Rocket Propulsion System; GG Cycle, Single Turbine



# Background: Ground Test Facility Run System (Simplified) Schematic



# The Cryogenic Propellant Tank



Net Result is densification of ullage gas which increases required mass flow rate of pressurant gas into tank (Assuming no change in mass flow rate and pressure vs. time profile at tank bottom discharge)

## Normal Operating Conditions:

- Tank walls and propellant are much colder than incoming pressurant gas
- Ullage gas temperature becomes much warmer than tank walls and propellant as pressurant gas enters and mixes with ullage gas and as ullage volume increases

## Ideally, there is:

- Uniform mixing of incoming pressurant gas with all gas in ullage region; and spatially uniform ullage gas temperature
- Negligible heat transfer between ullage gas and tank walls
- Negligible heat transfer between ullage gas and (cryogenic) propellant
- Negligible mass transfer between ullage gas and propellant

## In reality, there is:

- Moderately non-uniform mixing of incoming pressurant gas with gas in ullage region
- Non-uniform ullage gas temperature
- Significant heat transfer between ullage gas and tank walls
- Significant heat transfer between ullage gas and (cryogenic) propellant at least during times when the ullage gas volume is small
- Mass transfer between ullage gas and propellant significant effects under certain operating conditions

## **Collapse Factor Defined:**

- **Instantaneous**

**Collapse Factor: Actual Mass Flow Rate Divided by Ideal Mass Flow Rate of Pressurant Gas into Tank Ullage at a Particular Time**

- **Cumulative**

**Collapse Factor: Actual Total Mass Divided by Ideal Total Mass of Pressurant Gas Transferred into Tank Ullage**

**Table 1 Selected Empirical Collapse Factor Data for Non-Hydrogen Propellant Tanks**

Reference Citation	Test Run #	Tank Volume (gallons)	Tank Shape	Prop.	Propellant Expulsion			Pressurant Gas			Notes	Empirical Collapse Factor
					Mass Flow Rate (lb/sec)	Vol. Flow Rate (gpm)	Time (sec)	Tank Press. (psia)	Species	Inlet Temp. (deg R)		
2	None	25	Cylindrical	LN	10.0 - 14.0	88.9 - 124.3	16	172.3 - 300.4	He	523 - 530	(1)	1.540
2	None	25	Cylindrical	LN	10.0 - 14.0	88.9 - 124.3	16	155.2 - 321.6	Steam/He	1938 - 2029	(1), (2)	1.510
3	0027A	2603	Sphere	LOX	340-382	2066 - 2338	47	4400 - 5550	GN	579 - 521	(3)	1.061 + 0.060
3	0029B	2603	Sphere	LOX	462-478	2768 - 2873	15.2	7600 - 8200	GN	579 - 531	(4)	1.054 + 0.054
4	36	489.5	Sphere	LCH <sub>4</sub>	3.62	61.5	389.2	49.3	He	407		1.769
4	41	489.5	Sphere	LCH <sub>4</sub>	3.625	61.5	390.3	49.5	He	407		2.431
4	40	489.5	Sphere	LCH <sub>4</sub>	2.332	39.5	598.5	49.5	He	596		2.423
4	6	489.5	Sphere	LCH <sub>4</sub>	2.244	38.1	632.8	49.5	GCH <sub>4</sub>	407		2.352
4	11	489.5	Sphere	LCH <sub>4</sub>	6.137	104.6	233.5	49.2	GCH <sub>4</sub>	608		2.550
4	99	489.5	Sphere	LCH <sub>4</sub>	3.823	65.1	377.7	49.5	GN	603	(5)	5.247
5	See Notes	11220	Oblate Spheroid	LOX	201.2	1267.4	478	~46	He	325	(10)	1.375
5	See Notes	94996	Oblate Spheroid	LOX	2230 - 2256	14047 - 14227	360	36 - 37.5	GOX	510	(11)	1.325 - 1.500
6	12B	2596	Oblate Spheroid	LOX	57.7	363.5	47	34	He	520		2.432
6	13A	2596	Oblate Spheroid	LOX	57.7	363.5	120	34	He	527		2.605
6	10	2596	Oblate Spheroid	LOX	57.7	363.5	415	34	He	255		1.304
6	14A	2596	Oblate Spheroid	LOX	57.7	363.5	242	40	He	525		1.961
7	?	59892	Multi-Cylinder	LOX	3767 - 3769	23740	114.5	60 - 80	GOX/GN	840 - 600	(6), (7), (8)	~1.700
7	?	10098	Cylindrical	LOX	1261	7943	70	68 - 76	GOX/GN	602 - 641	(7), (8)	~1.650
7	?	16.5	Cylindrical	LN	0.924	8.21	120	50	GN	530	(7)	~2.110
8	74	5000	Cylindrical	LN	30. - 525.	267. - 4729.	38	335. - 359.	GN	506 - 447		2.35 - 1.39
8	74	900	Sphere	LOX	10.2	61.5	26	8200 - 8300	GN	548 - 544	(9)	4.1 - 1.57

- Notes:
- (1) Assumed near constant ullage gas temperature and no GN in ullage for expulsion
  - (2) Tank pre-pressurized with helium prior to expulsion with steam as pressurant gas
  - (3) Time includes ~3 sec. main ramp up in propellant expulsion mass flow rate and tank pressure; indicated tank pressure and flow rates do not include this ramp up
  - (4) Time includes ~5 sec. main ramp up in propellant expulsion mass flow rate and tank pressure; indicated tank pressure and flow rates do not include this ramp up
  - (5) Data shows 69.3% of added GN pressurant gas dissolved into upper layer of LCH<sub>4</sub> propellant
  - (6) Multiple tanks with 4-each 70-inch diameter tanks connected to one-each central 105-inch diameter tank
  - (7) Collapse factors approximated using energy allocations for ullage gas; insufficient data for more exact computations
  - (8) Tank pre-pressurized with GN prior to using GOX for propellant expulsion
  - (9) Only last 26-seconds of 38-second run has reliable data
  - (10) Propellant expulsion flowrate based on assumed 10% initial ullage and complete emptying of propellant from tank; test run is from unpublished document cited in Ref. 5
  - (11) Tank pressure and LOX expulsion rate obtained from Ref. 9 using average summations of LOX flow rate to 5-each J-2 engines on S-II stage; test run is from unpublished document cited in Ref. 5
- = Maximum Values  
 = Minimum Values  
 = High Subcritical & Other Supercritical Pressures

= Maximum Values
  = Minimum Values
  = High Subcritical Pressures

**Table 2 Selected Empirical Collapse Factor Data for Hydrogen Propellant Tanks (Continued on Next Page)**

Reference Citation	Test Run #	Tank Volume (gallons)	Tank Shape	Prop.	Propellant Expulsion				Pressurant Gas			Empirical Collapse Factor
					Mass Flow Rate (lb/sec)	Vol. Flow Rate (gpm)	Time (sec)	Tank Press. (psia)	Species	Inlet Temp. (deg R)	Notes	
3	004A	5002.5	Sphere	LH	78 - 108	6100 - 8560	34	7450 - 8200	GH	619 - 549	(1)	1.047 ± 0.037
5	See Notes	49,472	Sphere	LH	60.84	6140.5	296	91.7	GH	530	(16)	1.64
5	See Notes	246,840	Multi-Cylinder	LH	391.4 - 394.1	39696 - 39970	360	28.5 - 30.0	GH	200	(7), (16)	1.15 - 1.25
10	B-1	12	Cylindrical	LH	Not Given	Not Given	62.4	39.25	GH/He	330	(2)	3.42
10	B-2	12	Cylindrical	LH	Not Given	Not Given	62.4	39.25	GH/He	265	(2)	2.16
10	B-1	12	Cylindrical	LH	No Expulsion	N/A	N/A	14.7 - 44.25	GH	505		4.45
10	B-1	12	Cylindrical	LH	No Expulsion	N/A	N/A	14.7 - 61.75	GH	295		3.26
10	2	500	Cylindrical	LH	2.561	259.4	100	45.5	GH	320	(3), (4)	2.23
10	5	500	Cylindrical	LH	2.031	205.7	99	45.5	He	300	(3), (4)	1.72
10	7	500	Cylindrical	LH	2.031	205.7	105	49.3	GH	300	(3), (5)	1.74
10	10	500	Cylindrical	LH	1.833	185.7	111	45	GH	300	(3)	1.74
11	3	~370	Cylindrical	LH	0.939	95.1	197	44.1	He	450	(6)	0.878; 0.997
11	6	~370	Cylindrical	LH	0.47	47.6	351	44.1	He	450	(6)	0.908; 1.033
11	9	~370	Cylindrical	LH	0.624	63.3	352	29.4	He	450	(6)	1.043; 1.187
11	10	~370	Cylindrical	LH	0.939	95.1	211	44.1	He	180	(6)	0.48; 0.527
11	11	~370	Cylindrical	LH	0.939	95.1	214	44.1	GH	180	(6)	1.267; 1.277
12	1	500	Cylindrical	LH	2.995	303.4	89	45.5	GH	300	(4), (17)	1.56
12	2	500	Cylindrical	LH	2.388	262.1	103	47.6	GH	520	(4), (17)	2.23
12	3	500	Cylindrical	LH	2.22	224.8	120	46.5	GH	300	(4), (17)	1.8
12	5	500	Cylindrical	LH	2.694	272.90	99	45.5	He	300	(4), (17)	1.72
13	?	461.5	Sphere	SLH	1.478	131	190	50	GH	520	(8)	2.568
13	?	461.5	Sphere	SLH	0.552	48.9	510	25	GH	620	(8)	10.34
13	?	461.5	Sphere	SLH	0.668	59.2	420	50	GH	620	(8)	5.973
14	2 of Ref. 33	210	Cylindrical	LH	1.062	106.6	93	161	GH	210		2.12
14	3 of Ref. 33	210	Cylindrical	LH	0.346	35	284	57	GH	170		3.88
14	8 of Ref. 33	210	Cylindrical	LH	1.161	116.6	90	159	He	161		2.14
14	10 of Ref. 33	210	Cylindrical	LH	0.311	31.6	309	40	He	148		5.1
15	4 - 11	600	Horizontal Cyl	LH	0.56	57	420	27.5	GH	480 - 549	(9)	1.2 - 1.25
15	3	600	Horizontal Cyl	LH	0.31	31	1220	35	GH	480 - 549	(9)	4.32
15	7	600	Horizontal Cyl	LH	1.56	157	340	115	GH	480 - 549	(9)	1.67
15	9	600	Horizontal Cyl	LH	2.48	250	560	115	GH	480 - 549	(9)	2.20
15	5	600	Horizontal Cyl	LH	2.53	256	450	65	GH	480 - 549	(9)	2.52
15	6	600	Horizontal Cyl	LH	0.84	85	410	65	GH	480 - 549	(9)	1.80
16		489	Sphere	LH	2	202	130	50	GH	500		~2.38
16		489	Sphere	LH	0.5	50.6	522	50	GH	500		~3.33
16		8604	Sphere	LH	10.3	1043	446	50	GH	500		~2.29
16		8604	Sphere	LH	4.33	438	1060	50	GH	500		~2.86
16		489	Sphere	LH	1.89	191	138	50	GH	540		~2.76
16		8604	Sphere	LH	10	1012	459	50	GH	600		~2.33
17	7	489	Sphere	LH	0.65	65.9	453.4	50	GH	481 - 517	(10)	~2.86
17	10	489	Sphere	LH	1.86	187.9	193.2	50	GH	481 - 517	(10)	~2.53

= Maximum Values  
   = Minimum Values  
   = Other High Collapse Factors

**Table 2 Selected Empirical Collapse Factor Data for Hydrogen Propellant Tanks (Continuation from Previous Page)**

Reference Citation	Test Run #	Tank Volume (gallons)	Tank Shape	Prop.	Propellant Expulsion				Pressurant Gas			Empirical Collapse Factor
					Mass Flow Rate (lb/sec)	Vol. Flow Rate (gpm)	Time (sec)	Tank Press. (psia)	Species	Inlet Temp. (deg R)	Notes	
17	12	489	Sphere	LH	0.77	77.5	393.2	50	GH	481 - 517	(10)	~3.03
17	14	489	Sphere	LH	0.92	92.9	337	50	GH	481 - 517	(10)	~2.94
17	15	489	Sphere	LH	1.32	133.9	249.7	50	GH	481 - 517	(10)	~2.70
17	83	489	Sphere	LH	0.67	67.5	428.8	50	GH	481 - 517	(10)	~3.20
17	84	489	Sphere	LH	0.98	98.8	307.6	50	GH	481 - 517	(10)	~2.73
17	85	489	Sphere	LH	1.91	193	174.4	50	GH	481 - 517	(10)	~2.58
18	4	8604	Sphere	LH	9.60	972	531.6	50	GH	302	(10)	1.85
18	7	8604	Sphere	LH	4.28	433	1119.3	50	GH	302	(10)	2.07
18	8	8604	Sphere	LH	4.66	472	1037.2	50	GH	303	(9), (10)	2.07
18	15	8604	Sphere	LH	10.07	1019	509.3	50	GH	540	(10)	2.60
19	5	1291	Oblate Spheroid	LH	0.60-0.65	66.3	2160	54.6	GH	491	(11), (15)	5.222
19	5 R	1291	Oblate Spheroid	LH	0.38-0.40	66.3	1680	54.7	GH	491	(12), (13)	5.333
19	6	1291	Oblate Spheroid	LH	0.60-0.65	40.8	2280	54.9	GH	491	(13), (15)	5.0
19	9	1291	Oblate Spheroid	LH	0.60-0.65	66.3	1620	55.0	GH	594	(14), (15)	4.933
20	506	1291	Oblate Spheroid	LH	~0.83	83.6	760	33.9	GH	529		2.46
20	507	1291	Oblate Spheroid	LH	~0.58	58.5	1086	44.3	GH	531		2.568
20	508	1291	Oblate Spheroid	LH	~0.32	32.2	1974	44	GH	533		2.58
20	509	1291	Oblate Spheroid	LH	~0.84	84.7	741	54.3	GH	535		2.85
20	510	1291	Oblate Spheroid	LH	~0.58	58.2	1089	54.9	GH	531		2.74
20	511	1291	Oblate Spheroid	LH	~0.32	32.1	1978	55.1	GH	526		2.86
21	?	489	Sphere	SLH	~0.55	52.3	505	35	He	540	(8)	3.788
21	?	489	Sphere	SLH	~1.26	120.0	220	35	He	540	(8)	3.178
21	?	489	Sphere	SLH	~0.54	51.8	510	35	He	250	(8)	2.100
21	?	489	Sphere	SLH	~1.38	132.0	200	35	He	250	(8)	1.591
21	?	489	Sphere	SLH	~0.58	55.0	480	35	He/GH	540	(2), (8)	6.655
21	?	489	Sphere	SLH	~1.32	125.7	210	35	He/GH	540	(2), (8)	3.727

- Notes:
- (1) Time includes ~12 sec. main ramp up of tank pressure; indicated flow rates are at main stage after this ramp up
  - (2) Pre-pressurized with helium followed by expulsion with hydrogen pressurant gas
  - (3) Propellant expulsion flow rates approximated by scaling of tank geometry drawings, given initial ullage height, liquid level change in tank with a associated time span; Collapse Factor data also reported in Ref. 14
  - (4) Horizontal sloshing in tank at 0.5-Hz and 0.5-inch amplitude throughout expulsion
  - (5) Horizontal sloshing in tank at 0.5-Hz and 0.5-inch amplitude for last 85-seconds of expulsion
  - (6) Two collapse factors; first based on constant ullage gas temperature and pressure throughout expulsion; second based on saturated GH vapor in ullage at one atmosphere before tank pressurization
  - (7) Propellant mass flow rate data obtained from average LH propellant consumption of 5-each J-2 rocket engines on Saturn launch vehicle S-II stage from Ref. 9; tank pressure also obtained from this reference
  - (8) SLH is slush hydrogen, mixture of solid and liquid hydrogen
  - (9) Pressurant gas inlet temp. not reported; est. based on description of test apparatus and procedures
  - (10) Initial 30 to 56 sec. of the total time is tank pressurization and hold prior to propellant expulsion
  - (11) Submerged injection of pressurant gas, 21 min. tank pressurization, 15 min. CLH expulsion
  - (12) Submerged injection of pressurant gas, 13 min. tank pressurization, 15 min. CLH expulsion
  - (13) Submerged injection of pressurant gas, 13 min. tank pressurization, 25 min. CLH expulsion
  - (14) Submerged injection of pressurant gas, 12 min. tank pressurization, 15 min. CLH expulsion
  - (15) Initial 12- to 21-minutes of the total time is tank pressurization and hold prior to propellant expulsion
  - (16) Test runs are from unpublished report cited in Ref. 5
  - (17) Test run nos. are from another document cited in Ref. 12

- **Vertical Temperature Gradient in Ullage Gas Region**
  - Significant Effects on Collapse Factor
  - Fluid Density and Transport Properties Affected by Temperature
  - Pressure Distribution (Caused by Elevation Head) has Negligible Effects
- Vertical Temperature Gradients Measured Empirically in Some Studies
  - Limited to Low Subcritical Tank Pressures
  - Instrument Rakes Damaged or Destroyed at Higher Tank Pressures
- Ullage Gas Region Vertical Temperature Gradients, Empirical Data (Next Slide)



Table 3. Selected References Containing Empirical Ullage Gas Region Vertical Temperature Distribution/Gradient Data

Reference Citation	Test Number	Prop.	Press. Gas	Press. Gas Inlet Temp. (deg R)	Prop. Expul. Time (sec)	Ullage Gas Region Vertical Temp. Gradient (deg R)	
						Min.	Max.
Lockheed Report ER-5238 (1961)	3	LH	GH	300	120	?	218.5
Lockheed Report ER-5238 (1961)	5	LH	He	300	99	?	223.5
Lockheed Report ER-5238 (1961)	7	LH	GH	300	111	?	255.5
Arnett and Voth (1972)	B-2	LH	N/A	N/A	N/A	80.1	126
Baral (1988)	(Fig. 4)	LOX	GOX	540	100	288	333
Bouregal (1968)	1	LH	He	450	217	342	405
Bouregal (1968)	3	LH	He	450	197	351	405
Bouregal (1968)	7	LH	He	450	375	405	405
Bouregal (1968)	11	LH	GH	180	214	149.4	193
Bowersock, et al. (1960)	RT-3	LN	GN	~520	175	140	195
Cady, et al. (1990)	2.0-6	TPH	GH	540	~980	193	238
Cady, et al. (1990)	2.0-8	TPH	He/GH	144 and 540	~870	180	211
Clark (1965)	130-15 in Ref. 2	LOX	He	500 - 605	120	380	405
Coxe and Tatum (1962)	1 (Fig. 5)	LH	GH	300	89	~223.5	~248.5
DeWitt and McIntire (1974)	8	LCH <sub>4</sub>	GCH <sub>4</sub>	400	231	?	174.6
DeWitt and McIntire (1974)	6	LCH <sub>4</sub>	GCH <sub>4</sub>	400	633	?	176.4
DeWitt and McIntire (1974)	11	LCH <sub>4</sub>	GCH <sub>4</sub>	600	234	?	369
DeWitt and McIntire (1974)	37	LCH <sub>4</sub>	He	400	223	?	211
DeWitt and McIntire (1974)	42	LCH <sub>4</sub>	He	600	224	?	380
DeWitt and McIntire (1974)	63	LCH <sub>4</sub>	GH	400	219	?	193
DeWitt and McIntire (1974)	68	LCH <sub>4</sub>	GH	600	222	?	398
Hasan, et al. (1991)	?	LH	N/A	N/A	14400	5.4	49.5
Hasan, et al. (1991)	?	LH	N/A	N/A	14400	4.5	48.6
Kendle (1970)	?	LH	GH	~525	130	?	~475
Kendle (1970)	?	LH	GH	~525	130	?	~435
Kendle (1970)	?	LH	GH	~525	130	?	~245
Nein and Thompson (1965)	130-6	LOX	GOX	540	150	302	372
Nein and Thompson (1965)	130-9	LOX	GOX	370	150	147	207
Roudebush (1965)	Ex. 1	LH	GH	488-525	90	?	428
Roudebush (1965)	Ex. 1	LH	GH	488-525	178	?	428
Roudebush (1965)	Ex. 1	LH	GH	488-525	320	?	428
Roudebush (1965)	Ex. 2	LH	GH	480-515	93	?	436
Roudebush (1965)	Ex. 3	LH	GH	375-520	284	?	450
Roudebush (1965)	Ex. 4	LH	GH	450-580	101	?	455
Roudebush (1965)	Ex. 5	LH	GH	395-273	95	?	208
Roudebush (1965)	Ex. 6	LH	GH	380-630	88	?	575
Roudebush (1965)	Ex. 7	LH	He	525-535	355	?	475
Roudebush (1965)	Ex. 8	LH	He	525-530	90	?	475
Roudebush (1965)	Ex. 9	LH	He	325-215	100	?	165
Roudebush (1965)	Ex. 10	LH	He	350-610	309	?	597
Stochl, et al (1970) NASA TN-D-5621	88	LH	GH	331	396	?	250
Stochl, et al (1970) NASA TN-D-5621	85	LH	GH	488	137	?	445
Stochl, et al (1970) NASA TN-D-5621	97	LH	GH	603	134	?	650
Stochl, et al (1970) NASA TN-D-7019	4	LH	GH	306	478	?	247
Stochl and DeWitt (1969)	?	LH	GH	520	278	?	~460
Stochl and DeWitt (1969)	?	LH	GH	520	278	?	~305
Swalley (1966)	AS-203 (Saturn IB Launch 7/66)	LH	N/A	N/A	22,498	7	195
Van Dressar and Stochl (1993)	509	LH	GH	531	1110	245	423
Van Dressar and Stochl (1993)	510	LH	GH	529	741	?	405
Van Dressar and Stochl (1993)	511	LH	GH	526	1978	?	392

## • Horizontal Temperature Gradient in Ullage Gas Region

- Known to Exist from Empirical Data
- Temperature Probe Rakes and Instruments on Inner or Outer Tank Wall
- Most of Gradient Appears to be in Thin Boundary Layer Near Tank Wall, but little or no Empirical Data to Validate or Support
- Empirical Data Limited to Low Subcritical Pressure Cases
- Selected Tabular Empirical Data:

Table 4. Selected Empirical Ullage Gas and Adjacent Tank Wall Temperature Data for Approximations of Ullage Gas Region Horizontal Temperature Gradients

Reference Citation	Test Number	Prop.	Press. Gas	Press. Gas Inlet Temp. (deg R)	Expul. Time (sec)	Horizontal Temperature Gradient, Tank Vertical Centerline to Tank Wall (deg R)	
						Minimum	Maximum
Lockheed Report ER-5238 (1961)	3	LH	GH	300	120	0	~63
Lockheed Report ER-5238 (1961)	4	LH	GH	300	87	4.5	~72
Lockheed Report ER-5238 (1961)	5	LH	He	300	99	0.5	51
Lockheed Report ER-5238 (1961)	6	LH	He	300	95	26	95
Lockheed Report ER-5238 (1961)	7	LH	GH	300	111	9	71
Bourgarel, et al. (1968)	4	LH	He	450	205	9	107
Bourgarel, et al. (1968)	7	LH	He	450	375	0	130
Bourgarel, et al. (1968)	9	LH	He	450	352	~5	126
Bourgarel, et al. (1968)	11	LH	He	180	214	0	59
Bowersock, et al. (1960)	19	LN	GN	?	N/A	0	107
Coxe and Tatom (1962)	1	LH	GH	300	89	0	99
DeWitt and McIntire (1974)	8	LCH <sub>4</sub>	GCH <sub>4</sub>	400	231	0	117
DeWitt and McIntire (1974)	6	LCH <sub>4</sub>	GCH <sub>4</sub>	400	633	0	80
DeWitt and McIntire (1974)	11	LCH <sub>4</sub>	GCH <sub>4</sub>	600	234	0	281
DeWitt and McIntire (1974)	37	LCH <sub>4</sub>	He	400	223	0	97
DeWitt and McIntire (1974)	42	LCH <sub>4</sub>	He	600	224	0	180
DeWitt and McIntire (1974)	63	LCH <sub>4</sub>	GH	400	219	2	99
DeWitt and McIntire (1974)	68	LCH <sub>4</sub>	GH	600	222	0	225
Hasan, et al. (1991)	?	LH	N/A	N/A	N/A	1	29
Roudebush (1965)	Ex. 1	LH	GH	488 - 520	350	15	220
Roudebush (1965)	Ex. 4	LH	GH	450 - 580	101	0	300
Roudebush (1965)	Ex. 6	LH	GH	385 - 630	88	0	415
Roudebush (1965)	Ex. 8	LH	He	524 - 530	90	~20	270
Stochl, et al. (1970), NASA TN-D-7019	4	LH	He	306	478	2	55
Stochl, et al (1970) NASA TN-D-5621	88	LH	He	331	396	2	100
Stochl, et al (1970) NASA TN-D-5621	85	LH	He	488	137	19	282
Stochl, et al (1970) NASA TN-D-5621	87	LH	He	603	134	0	540

- Vertical Temperature Gradients in the Cryogenic Propellant Region Can Affect Collapse Factor, But to a Much Lesser Extent than Vertical Temperature Gradients in the Ullage Gas Region
  - Pressure gradients in the propellant region are higher than those in the ullage gas region, but have negligible effects on fluid density and other properties
  - Empirical data for cryogenic (liquid) propellant vertical temperature gradients are much more extensive than data for ullage gas vertical temperature gradients
- Vertical temperature gradients in propellant region range from 5 to 30 R
- Most of the gradient is in the Upper 2 to 20% of Initial Propellant Region Height
  - 3-in. to 3-ft. depth below liquid surface for larger tanks
  - Less than 6" height for smaller tanks
- Prior studies with Vertical Temperature Gradients in Propellant Region (Next Slide)

Table 5. References with Empirical Propellant Vertical Temperature Gradient/Profile Data

Reference Citation	Test Number	Prop.	Press. Gas	Propellant Height (ft.)		Press. Hold or Expul. Time (sec.)	Tank Press. (psia)
				Minimum	Maximum		
Lockheed Report - ER-5238 (1981)	3	LH	GH	1	7.25	120	46.5
Lockheed Report - ER-5238 (1981)	4	LH	GH	0.08	6.75	87	46.6
Al-Najem, et al. (1993)	3L/min	Water	*	1.31	3.11	840	~14.7
Al-Najem, et al. (1993)	15L/min	Water	*	1.31	3.11	180	~14.7
Barnett (1967)	2	LN	N/A	3.17	3.17	60	39.7
Barnett (1967)	2	LN	N/A	3.17	3.17	360	29.7
Barnett (1967)	3	LN	N/A	3.17	3/17	60	29.7
Barnett (1967)	3	LN	N/A	3.17	3.17	360	29.7
Barnett, et al. (1964)	4	LH	He	13.17	13.17	119	18.7-32.7
Barnett, et al. (1964)	4	LH	He	13.17	13.17	119	18.7-32.7
Barnett, et al. (1964)	Fig. 8	LH	GH	4.75	4.75	100	?
Barnett, et al. (1964)	Fig.8	LH	GH	4.75	4.75	600	?
Coxe and Tatom (1962)	2	LH	GH	<0.50	7.46	103	47.6
Coxe and Tatom (1962)	5	LH	He	<0.50	7.51	99	45.5
Coxe and Tatom (1962)	6	LH	GH/He	<0.50	7.63	95	47.0
Coxe and Tatom (1962)	7	LH	GH	<0.50	7.33	111	45.0
Coxe and Tatom (1962)	10	LH	GH	<0.50	7.39	105	45.5
DeWitt and McIntire (1974)	9	LCH <sub>4</sub>	GCH <sub>4</sub>	~0.85	~4.15	638	48.6
DeWitt and McIntire (1974)	10	LCH <sub>4</sub>	GCH <sub>4</sub>	~0.85	~4.15	410	48.9
DeWitt and McIntire (1974)	11	LCH <sub>4</sub>	GCH <sub>4</sub>	~0.85	~4.15	234	49.2
DeWitt and McIntire (1974)	97	LCH <sub>4</sub>	GN	~0.85	~4.15	568	49.5
DeWitt and McIntire (1974)	98	LCH <sub>4</sub>	GN	~0.85	~4.15	232	49.5
Fan, et al (1969)	13	LN	GN	1.98	1.98	7200	450
Ghaddar, et al. (1989)	6.5L/min	Water	*	5.25	6.56	1500	~14.7
Ghaddar, et al. (1989)	9L/min	Water	*	5.25	6.56	1500	~14.7
Gursu, et al. (1993)	B-2	LH	N/A	6.02	6.02	40	16.5 - 17.4
Gursu, et al. (1993)	B-2	LH	N/A	6.02	6.02	152	16.5 - 19.5
Hasan, et al. (1991)	?	LH	N/A	4.59	4.59	14,400	14.7 - 18.4
Hasan, et al. (1991)	?	LH	N/A	4.59	4.59	43,200	14.7 - 27.0
Kharin, et al. (1991)	?	LH	N/A	3.75	8.52	20,700	19.15
Liebenburg and Edeskuty (1965)	?	LH	N/A	18.47	18.47	136,800	18.7 - 39.1
Neff and Chiang (1967)	17	LH	N/A	3.91	3.91	120	~27
Neff and Chiang (1967)	19	LH	N/A	1.38	1.38	400	~31.2
Neff and Chiang (1967)	40	LN	N/A	3.97	3.97	160	~18.0
Neff and Chiang (1967)	38	LN	N/A	1.27	1.27	700	~18.9
Olsen (1966)	1	LH	GH	2.5	2.5	600	54.7
Olsen (1966)	3	LH	GH	2.5	2.5	720	22.7
Ordin, et al. (1960)	?	LH	GH	?	~2	600	14.7 - 55
Schmidt, et al. (1960)	A-3	LH	GH	4.19	4.19	900	125 - 160
Schmidt, et al. (1960)	B-1	LH	GH	3.98	3.98	104,400	15.5 - 24.7
Segel (1965)	?	LH	N/A	2.36	2.36	600	14.7 - 73.5
Segel (1965)	?	LH	N/A	2.21	2.21	600	14.7 - 73.5
Segel (1965)	?	LH	N/A	2.30	2.30	600	14.7 - 73.5
Segel (1965)	?	LH	N/A	2.14	2.14	600	14.7 - 73.5
Tanyun, et al. (1996)	?	LH	N/A	6.50	6.50	120	?
Tanyun, et al. (1996)	?	LH	N/A	6.50	6.50	300	?

- **Horizontal Temperature Gradients in Propellant Region**

- Empirical data is limited
- Data shows small horizontal temperature gradient in most cases
- All data indicates all or most of the gradient is in thin thermal boundary layer near the tank inner wall
- Propellant temperature is nearly equal to that of adjacent tank wall in nearly all cases

- **Multiple Fluid Species in Ullage Gas and Cryogenic Propellant Regions**

- Limited to Cases where pressurant gas species is different from cryogenic propellant species
  - Nitrogen pressurant gas over LCH<sub>4</sub> or LOX propellant
  - Helium pressurant gas over LH, LCH<sub>4</sub>, or LOX propellant
- Known to exist in both ullage gas and propellant regions
- Always have propellant species in near saturated vapor state in initial ullage region prior to tank pressurization
- Quantitative empirical data (distribution of species mass fractions) is limited to a few studies
- Most existing data and stated conclusions of prior studies indicate that virtually all mixing of pressurant gas species in the propellant region is near (no more than one or two inches below) the interface between ullage gas and propellant regions
  - One exception is in DeWitt and McIntire (1974) where nitrogen gas over liquid methane was tested
  - Other exceptions are found in studies where helium gas was bubbled up through LH or LOX propellant

- **Multiple Fluid Species in Ullage Gas and Cryogenic Propellant Regions (continued)**
  - Quantitative measurements for multiple species in ullage gas region show:
    - Increased mass fraction of propellant when traversing from top to bottom of region
    - High propellant mass fractions concentrated in and restricted to lowermost one to two foot height in ullage gas region or lowermost 5 to 15% of ullage volume
    - Above findings occur when:
      1. Only one gas species used for tank pressurization and propellant expulsion
      2. Pressurant gas inlet diffuser is designed to reduce or prevent mixing of pressurant and ullage gases
  - Supercritical and High Subcritical Tank Operating Pressures are expected to have minimal/negligible mass fraction of propellant throughout ullage gas region if diffuser design and operating conditions assure minimal forced mixing at ullage-gas-to-propellant interface
    - Not proven, but supported, by results of the few studies covering and presenting collapse factor data with tanks operating at high supercritical pressures.

- **Other Effects on Collapse Factor:**

- Temperature Distribution Through Thickness of Tank Wall

- Treated as uniform for all but a few studies
- Tank wall temperature distribution is not directly determined with direct temperature instrumentation measurements in any study
- Selected studies use directly measured outer tank wall surface temperatures
- Small minority of studies use directly measured inner tank wall surface temperatures
- Tank wall less than ½-inch thick in all these studies
- Assumption of uniform temperature through the tank wall appears to be valid analytical approach that adds slight conservatism (increases) to collapse factor results
- The assumption is probably not valid for thick walled tanks and expected to yield overly conservative results
- One study for thick walled tanks operating at high supercritical pressures models inner 30% of wall thickness at uniform temperature with remaining 70% treated as an adiabatic boundary
- Two studies for thick walled tanks operating at high supercritical pressures use numerical-finite-difference method with temperature dependent wall material properties

- **Other Effects on Collapse Factor (continued):**
  - Pressurant Gas Entry Effects
    - Direction and Magnitudes of Velocity Vectors at Locations where Pressurant Gas Enters the Ullage
    - The Major Effect on:
      1. Temperature gradients in ullage gas region (previously described)
      2. Heat transfer across all ullage gas region boundaries
      3. Mass transfer across interface between ullage gas and propellant
    - Lesser effects on heat transfer across propellant region boundaries
    - As a Result, Pressurant Gas Entry Effects Have the Predominant Influence on Collapse Factors
    - Configuration and Location of Pressurant Gas Inlet Diffuser can be Optimized to Reduce Collapse Factors
      1. Reduce magnitude of all velocity vectors; large total cross-section flow area (where pressurant gas enters the diffuser)
      2. Horizontal and/or upward direction of velocity vectors; away from ullage-gas-to-propellant interface
      3. Provide maximum velocity jet dispersion before impinging on or flowing along tank walls (increase distance between entry points and tank walls)
      4. Certain tank geometries and severe operating conditions can limit attainable reduction in collapse factors



- **Analytical Methods and Models to Predict Collapse Factor**

- “Saturation Rule”

- Ullage gas density based on temperature equal to saturation temperature of cryogenic liquid (propellant)
- Ullage gas is at saturated vapor density if ullage and pressurant gas are same species as cryogenic liquid
- Good to very good results in some cases when compared to empirical results, but often overly conservative over-predicting by factors as high as ten

- Modifications and Enhancements to the “Saturation Rule”

- “Worst Case Rule” and “Equivalent Mass Model”
- Addition of assumptions and basic heat transfer correlations and approximations to reduce excessively high conservatism in results
- “Equivalent Mass Model” provided 10% under-prediction to 12.8% over-prediction of collapse factor
- Studies limited to one horizontal cylindrical tank configuration and size

## • Analytical Methods and Models to Predict Collapse Factor (Continued)

### • Semi-Empirical Curve-Fit Models

- A single equation or simultaneous set of equations
- Ullage gas, incoming pressurant gas, propellant temperature, and tank wall properties used in equation(s)
- Constants and exponents derived from empirical data developed and used in equation(s)
- Model presented in two studies, Epstein and Anderson (1968) and Epstein (1965), had collapse factor prediction errors below 12%, most errors around 5 to 6%
- Enhancements made, VanDresar (1995), to models from above two studies
  - Equivalent dimension parameters developed for spherical and oblate spheroid tanks
  - Revised constants for liquid hydrogen propellant expulsions
  - Methods added to adjust for cases with initial ullage volumes <20%, large final propellant volumes, and internal tank hardware

- **Analytical Methods and Models to Predict Collapse Factor (Continued)**

- Upper and Lower Bound Analyses

- Developed in mid-1980's through early 1990's
- Major focus to evaluate pressurant gas requirements (collapse factors) at supercritical and high subcritical tank pressures
  - Accommodate no distinction between liquid and gas phases or possibility of two-phase region
- Upper bound based on complete mixing of all fluids in tank
- Lower bound based on separate ullage gas and cryogenic propellant regions with no heat or mass transfer at boundaries (except where pressurant gas enters the ullage and cryogenic propellant is discharged)
  - Ullage-gas-to-propellant interface modeled as horizontal plane
- Empirical collapse factor data always fell between the upper and lower bound collapse factor data (but this was often a very wide range)

- Lumped Mass Fluid Region (LMFR) Models  
(presented on following slides)

- Multiple Discrete Fluid Segment (MDFS) Models  
(presented on slides that follow those for LMFR Models)

**Table 6 Summary Data for Lumped Mass Fluid Region (LMFR) Models**

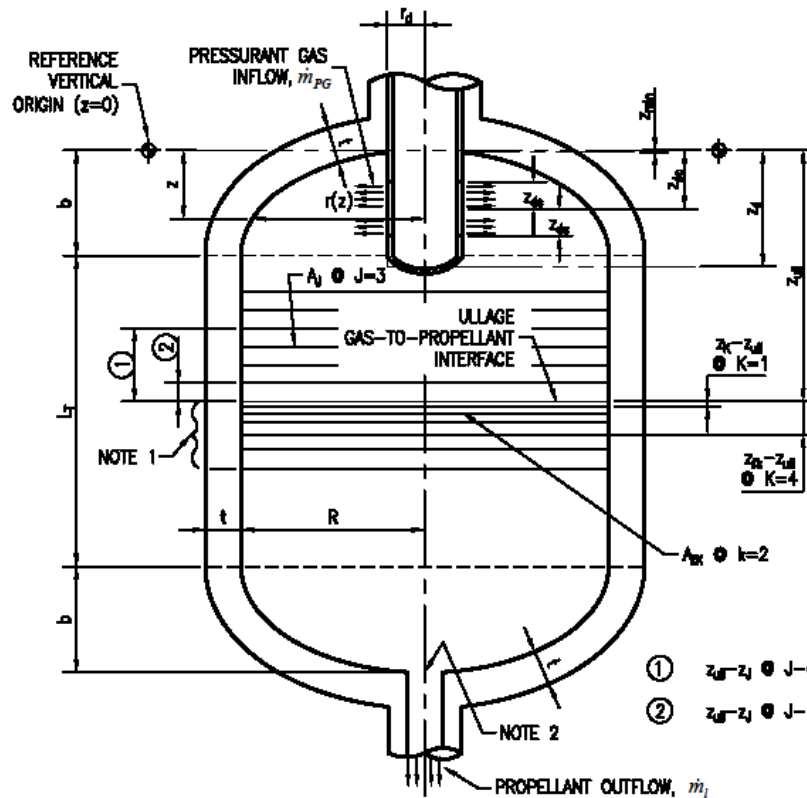
Year	Reference Citation	Heat Transfer				Mass Transfer	Model Errors Compared to Empirical Data
		Ullage Gas to Wall	Propellant to Wall	Ullage Gas to Propellant	External Tank Wall	Ullage Gas to Propellant	
1962	12	NLC, Correlation for Conv. H.T. Coeff. not provided	Based on H.T. from wall boiling liquid propellant	Not Discussed	NLC, Correlation for Conv. H.T. Coeff. not shown	Not Discussed	Range: -9.6 to 7.8%; Mean: 1.11%; Std. Dev. 5.0%; 10 Tests Compared
1965	14	NLC, NC, Note 7	Assumed Negligible	Assumed Negligible	Not Discussed	Assumed No Mass Transfer	Range: -10.4 to 18.5%; Mean: 0.65%; Std. Dev. 7.74%; 18 Tests Compared
1962	33	NLC, NC, Note 9	Assumed Negligible	Not Modeled	Modeled as Adiabatic	Determined from Empirical Data	Range: -9.0 to 8.4%; Mean: 0.34%; Std. Dev. 4.57%; 12 Tests Compared
1992	79	NLC, NC, VP & HP [Ref. 87 Correlations]	NLC, NC, VP & HP [Ref. 87 Correlations]	NLC, NC, HPCSU [Ref. 87 Correlations]	Modeled as Adiabatic	Assumed Negligible	Pressurant gas supply bottle press. And temp. show < 1 K and <0.5 MPa error for part of Test 74 on E-8 Test Stand
1989	80	NLC, NC & FC, Notes 3 and 5 [Ref. 34 Correlations]	Assumed Negligible	NLC, NC & FC, Notes 3 and 6 [Ref. 34 Correlations]	Modeled as Adiabatic, Note 5	None, equivalent mass transfer modeled by added H.T., Note 6	No comparisons presented; model predicts Collapse Factor of 1.20 to 1.24
1961	88	Notes 1 and 3	Note 2	Note 4	Note 1	Note 1	Range: -9.3 to 13.1%; Mean: 2.75%; Std. Dev. 5.74%; 11 Tests Compared
1967	89	NLC, NC	NLC, NC	Not Discussed	Not Discussed	Not Discussed	~10 to 12% estimated from UG Press. & Temp. data
1998	90	NLC, NC, HPCSD	EC	NLC, NC, HPCSU	Not Discussed	Not Discussed	~18 to 30% based on comparison with model data in Epstein and Anderson (1968)
1964	91	NLC, NC, Note 7	Assumed Negligible	NLC, NC, HPCSU [from Ref. 92]	Not Discussed	(1) and (2)	-14.1, 4.7, -1.8, 0% for GH over LH; -2.5, -8.7, 6.7, -2.5% for GHe over LH
1964	92	NLC, NC, VP & FC	NLC, NC, VP & HP, FC	NLC, NC, HPCSU	NLC, FC & Radiation	(1), (6), and Note 8	No Comparisons Presented

Key:

- NLC = Newton's Law of Cooling
- NC = Natural (Free) Convection
- FC = Forced Convection
- HP = Horizontal Plate (Natural Convection Correlations)
- HPCSD = Horizontal Plate (Natural Convection Correlations), Cold Side Down
- HPCSU = Horizontal Plate (Natural Convection Correlations), Cold Side Up
- VP = Vertical Plate (Natural Convection Correlations)
- EC = Equivalent Conduction; thermal conductivity and slope of temperature gradient across finite segment/element at boundary
- (1) = First Mass Transfer Computation Technique, from "Mass Transfer Correlations" section of Chapter II of Ref. 3
- (2) = Second Mass Transfer Computation Technique, from "Mass Transfer Correlations" section of Chapter II of Ref. 3
- (6) = Sixth Mass Transfer Computation Technique, from "Mass Transfer Correlations" section of Chapter II of Ref. 3

- Notes:
1. An energy balance equation using propellant, mean ullage gas, entering pressurant gas, and tank wall temperatures; temperature differentials; and empirically determined coefficients is used to calculate rate of change of ullage gas temperature at discrete time steps.
  2. A condensation or evaporation energy balance equation, whichever has highest magnitude, using propellant, mean ullage gas, and tank wall temperatures; temperature differentials; and empirically determined coefficients is used to calculate rate of change of liquid propellant temperature at discrete time steps.
  3. Ullage gas is divided into two regions; the lower region contains only the initial mass of ullage gas prior to entry of pressurant gas and the upper region contains only pressurant gas supplied from external source.
  4. External tank heating is assumed to heat and evaporate liquid propellant only. Evaporation rate of propellant is calculated from heat transfer equation using tank wall and liquid propellant temperatures, heat transfer areas, latent heat of vaporization, and empirically determined coefficients.
  5. To simulate effects of transient and non-uniform temperatures through thick tank walls, the wall is modeled as having uniform temperature through 70% of the actual wall thickness where heat is transferred from the ullage gas; 30% of the wall thickness is modeled as thermally isolated from remaining wall.
  6. 740 BTU/hr-ft<sup>2</sup>-R for GH over LH and 520 BTU/hr-ft<sup>2</sup>-R for GN over LOX added to calculated convective heat transfer coefficient from Ref. 34 correlations to simulate effects of mixing between ullage gas and cryogenic propellant; these resulted in approximate 10% increase in required pressurant gas.
  7. Ullage gas modeled as having linear vertical temperature profile with temperature at top of region equal to entering pressurant gas temperature and temperature at bottom of region equal to saturation temperature of propellant; Mean ullage gas temperature used to calculate heat transfer at ullage gas boundaries with tank wall is average of temperatures at top and bottom of ullage gas region.
  8. During rapid change in tank pressure, mass transfer across ullage-gas-to-cryogenic-propellant interface is product of ullage volume and ullage gas density change based on net difference between new tank pressure and propellant saturation pressure.
  9. Natural convection correlation used with time of pressurant gas entry, thermal properties of ullage gas and tank wall, tank wall thickness and inside diameter to compute ratio of actual to maximum total heat in tank wall; Maximum total heat in tank wall is when all of tank wall is at temperature of the incoming pressurant gas; Coefficients and exponents in the correlation to compute ratio of actual to maximum total heat in tank wall are derived from curvefits of empirical data.

# Modeling the Cryogenic Propellant Tank System; the Higher Fidelity Multiple Discrete Fluid Segment (MDFS) Models



**NOTES:**

- 1. SLL=STRATIFIED LIQUID LAYER; REMAINING BULK LIQUID AT UNIFORM TEMP.
- 2. VORTEX BREAKER LOCATION, ASSUME NEGLIGIBLE VOLUME OF VORTEX BREAKER, ASSUME NEGLIGIBLE HEAT CAPACITANCE OF VORTEX BREAKER

OBLATE SPHEROID TANK IS SPECIAL CASE WITH  $L_T = \phi$  AND  $R > b$   
 SPHERICAL TANK IS SPECIAL CASE WITH  $R=b$  AND  $L_T = \phi$

Subdivide ullage gas into discrete vertically stacked segments to model vertical temperature distribution

Subdivide upper portion of cryogenic propellant region where most of vertical temperature gradient is expected

Variation of temperature in horizontal or radial direction limited to small boundary layer near the tank wall

**Table 7 Summary Data for Multiple Discrete Fluid Segment (MDFS) Models**

Year	Reference Citation	Heat Transfer					Mass Transfer			Model Errors Compared to Empirical Data
		Ullage Gas to Wall	Propellant to Wall	Ullage Gas to Propellant	Intra-Ullage-Gas Segment-to-Segment	Intra-Propellant Segment-to-Segment	External Tank Wall	Ullage Gas to Propellant	Intra-Ullage-Gas Segment-to-Segment	
2009	3	NLC, NC & FC	NLC, NC	NLC, NC, FC	EC & EFC	EC	Adiabatic Outer Wall Modeled	N/A, Assumed to be Zero	No Mass Transfer other than Pressurant Gas Entry	-13.0 to +1.0% for Test 004A +2.9 to +14.0% for Test 0027A -2.7 to +9.1% for Test 0029B
1970	17 and 18	NLC, NC	N/A, No Heat Transfer Assumed	NLC, NC (Same correlation as Ref. 91)	EC	N/A, Uniform Propellant Region Modeled	Adiabatic Outer Wall Modeled	(1)	No Mass Transfer other than Pressurant Gas Entry	Range: -2.73 to 19.48%; Mean: 5.29%; Std. Dev.: 5.56%; 19 Tests Compared
1988	23	NLC, NC	NLC, NC	EC	EC	EC	NLC, NC, Note 2	(1)	(6)	<5%
1965	30	NLC, NC	N/A, No Heat Transfer Assumed	NLC, NC	N/A, No Heat Transfer Assumed	N/A, Uniform Propellant Region Modeled	Input Heat Flux	N/A, Assumed to be Zero	No Mass Transfer other than Pressurant Gas Entry	Range: -8.23 to 12.04%; Mean: 2.22%; Std. Dev.: 6.05%; 10 Tests Compared
1966	34	NLC, NC & FC	NLC, NC	NLC, NC & FC	EC	EC	NLC, NC & Radiation, Note 1	(6)	(6)	Range: Approx. -30 to 12%; Mean: 0.1 to 2.3%; Std. Dev.: 10.9 to 8.5%; 11 Tests Compared
1992	93	No Heat Transfer Assumed	EC	EC (liquid side only)	N/A	EC	Input Heat Flux	(1)	N/A; Ullage Gas at Uniform Temp.	No Comparisons Presented
1963	94	NLC, NC & FC	NLC, NC	NLC, NC & FC	EC	EC	NLC, NC & Radiation, Note 1	(1) and (6)	(6)	Comparisons not presented; ~10% Max. Cumulative Error; ~20% Max. Instantaneous Error from Nein and Thompson (1966)
1965	95	NLC, NC & FC	NLC, NC	NLC, NC & FC	EC	EC	Unknown	(1)	Unknown	~10% for Test 130-9; ~10 to 12% for Test 130-6; ~5% for Test 6E
1974	96	NLC, NC & FC	No Heat Transfer Assumed	NLC, NC (Same correlation as Ref. 91)	EC	N/A, Uniform Propellant Region Modeled	Input Heat Flux	Not Discussed	No Mass Transfer other than Pressurant Gas Entry	0.5 to 16.0% Error for Tank Pressurization; 7.0 to 12.4% Error for Propellant Expulsion

Key:

NLC = Newton's Law of Cooling  
 NC = Natural (Free) Convection; Ref. 34 correlations unless noted otherwise  
 FC = Forced Convection; correlation presented in "Combined Natural and Forced Convection Correlations" section  
 EC = Equivalent Conduction; thermal conductivity and slope of temperature gradient across finite segment/element at boundary  
 EFC = Equivalent Forced Convection (and Mixing); similar to correlation presented in "Combined Natural and Forced Convection Correlations" section  
 (1) = First Mass Transfer Computation Technique, from "Mass Transfer Correlations" Section of Chapter II in Ref. 3  
 (6) = Sixth Mass Transfer Computation Technique, from "Mass Transfer Correlations" Section of Chapter II in Ref. 3

The MDFS Models had Errors Comparable to LMFR Models, but the MDFS Models Covered Wider Range of Tank Sizes, Pressures, and Expulsion Flow Rates

## Summary

- Wide Range of Empirical Collapse Factors; 0.87 to 10.34  
(Cannot directly apply empirical data to all cases without understanding parameters that cause the wide variations)
- For Majority of Cases, Empirical Collapse Factor Data at Low Subcritical Operating Pressures
- For Some Cases, Empirical Collapse Factor Data at Supercritical & High Subcritical Operating Pressures
- Significant Effects on Collapse Factors; Pressurant Gas Entry Velocity Vectors into Ullage which Drive Heat Transfer Rates at Ullage Gas Region Boundaries, Ullage Gas Vertical Temperature Gradients, Mass Transfer between Ullage Gas and Propellant Regions
- Many Types of Analytical Models for Collapse Factor Prediction
- MDFS (Multiple Discrete Fluid Segment) Models Provide best Predictions over Full Range of Operating Conditions